J. Euk. Microbiol., 46(2), 1999 pp. 174–193


# Morphology and Morphogenesis of *Metopus hasei* Sondheim, 1929 and *M. inversus* (Jankowski, 1964) nov. comb. (Ciliophora, Metopida)

WILHELM FOISSNER[1] and SABINE AGATHA

*Universität Salzburg, Institut für Zoologie, Hellbrunnerstrasse 34, A-5020 Salzburg, Austria*

ABSTRACT. The morphology and morphogenesis of *Metopus hasei* Sondheim, 1929 and *M. inversus* (Jankowski, 1964) n. comb. were investigated using live observation, silver impregnation, and scanning electron microscopy. *Metopus* has a spiral body organization and the ventral margin of the preoral dome bears five specialized ciliary rows, that form the so-called perizonal stripe. Division is homothetogenic, occurs in freely motile (i. e. non-encysted) condition, and includes a partial reorganization of the parental oral apparatus. During division, the complicated cell shape becomes ellipsoidal and all ciliary rows arrange meridionally. Stomatogenesis is entirely somatic (≅ pleurotelokinetal) and commences with the formation of kinetofragments in some dorsolateral kineties. The fragments become the opisthe's adoral membranelles, while the paroral membrane is generated by the left two perizonal ciliary rows, which proliferate kinetids intrakinetally. The perizonal stripe of the opisthe is generated by the three right parental perizonal kineties, which divide, and by two dorsolateral ciliary rows, which are added. The morphogenetic processes, especially the unique mode of formation of the paroral membrane, are used to define the order Metopida Jankowski, 1980 n. stat. more properly. The ontogenetic, ultrastructural, and sequence data available give no clear indication about metopid phylogeny, but definitely exclude metopids from the classical heterotrichs, with which they were classified for more than 100 years. Accordingly, we place the Metopida as incertae sedis in the subphylum Intramacronucleata Lynn, 1996.

**Supplementary key words.** Armophorida, Heterotrichida, Namibia, soil ciliates, stomatogenesis.

IT was a great surprise when in 1994 gene sequence data suggested some relationship between haptorid gymnostomes, such as *Spathidium,* and heterotrich metopids [14]. Morphologically and ecologically, there are hardly any obvious similarities between these groups. Haptorids have somatic monokinetids, a simple circumoral ciliary row, and are mostly aerobic predators, while metopids possess somatic dikinetids, conspicuous adoral membranelles, and are strictly anaerobic bacterivores [8, 26]. Accordingly, morphologists never considered a relationship between gymnostomes and metopids. Indeed, since Stein [48], they regarded metopids as typical heterotrichs (spirotrichs). In his classical study on sapropelic ciliates, Jankowski [31] presented an intriguing scenario of how metopids evolved from heterotrichs, such as *Blepharisma* and *Spirostomum.* His ideas were adopted and extended by most contemporary ciliatologists [8, 17, 44] and also influenced recent classifications [41], although Lynn and Small [37] now separated the heterotrichs at subphylum level from Jankowski's armophorids, in which they include the metopids [44].

The lack of any morphological support for a relationship of gymnostomes and metopids stimulated Hirt et al. [28] to reanalyse the sequence data from Embley and Finlay [14]. They found the strength of association to be highly dependent on the alignment and analysis method. Recently, however, Bernhard et al. [5] and Hammerschmidt et al. [27] supported Embley and Finlay [14] by investigating the small subunit rRNA gene sequences of two other representative haptorid gymnostomes, *Homalozoon* and *Loxophyllum.* And Lynn and Small [37] mentioned that SSrRNA sequences by Affa'a et al. (unpubl. data), demonstrate that armophorids (e. g. *Metopus*) and clevelandellids (e. g. *Nyctotherus*) form a clade that is the sister taxon of the Litostomatea (≅ gymnostomes, e. g. *Spathidium*). On the other hand, bootstrap values are low for the molecular *Metopus*-Haptorida-relationship, and recent trees [47, 51, 56] show paraphyly or no relationship at all. In this situation, it is certainly of considerable interest to know whether the sequence data are supported by ontogenetic features, which are a powerful means to unravel relationships between higher systematic categories [3, 7, 24]. Unfortunately, morphogenetic data are entirely lacking for metopids, while abundant and detailed investigations are available for haptorid gymnostomes [24]. We thus performed a study on the morphogenesis of two *Metopus* species, not only to investigate the basic ontogenetic pattern, but also the proposed relationships with haptorid gymnostomes or clevelandellid heterotrichs.

A further purpose of the present study is the detailed redescription of two *Metopus* species because alpha-taxonomy of metopids is extremely confused due to the often insufficient original descriptions and the lack of detailed redescriptions for most species. Accordingly, Esteban et al. [15] synonymized many species. However, this is probably not definite because metopids are poorly explored, possibly consisting of more species than presently assumed [11]. Part of the confusion is undoubtedly caused by insufficient documentation. For instance, the complicated body shape, which highly influences the recognition of taxa and their correct identification, has not yet been documented in all details in a single species. Thus, at the present state of knowledge, all species need abundant documentation by micrographs and careful drawings.

## MATERIALS AND METHODS

Two populations of *Metopus hasei* were studied in detail: the first was found in February 1994 in dry mud from rock-pools in the centre and at the bank of a temporary mountain river in the Aubschlucht near Bullsport, Namibia (16° 20′ E, 24° S); the second population was found in February 1995 in soil near a small lake on the Cape Peninsula (Sirkelsvlei), South Africa (18° 20′ E, 33° 50′ S). Data were supplemented by populations from Venezuela (rock-pools near Puerto Ayachucho) and Austria. *Metopus inversus* occurred in soil from the margin of a pool communicating with a nearby stream in the Aubschlucht near Bullsport, as described above.

Samples were air-dried for about four weeks and sealed in plastic bags. When the study commenced, ciliates were reactivated from the resting cysts by the non-flooded Petri dish method [20]. Briefly, this simple method involves filling a Petri dish (10–15 cm in diameter) with terrestrial material (litter, soil, and moss) and saturating but not flooding it with distilled water. Such cultures were analysed for ciliates by inspecting about 2 ml of the run-off on d 2, 7, 14, 21, and 28. *Metopus* spp. developed when oxygen was depleted in the bottom of the cultures. Dividers were rare, as is usual in such raw cultures. They are, however, also rare in pure cultures, possibly because some species divide in cysts [15].

Morphological methods used are described in [21]. Specifically, silver carbonate impregnations were made in the following way to exclude any confusion with other species present in

[1] To whom correspondence is addressed. Telephone: +49 (0) 662 8044-5615; FAX: +49 (0) 662 8044-5698.

the raw cultures: individual cells were picked up with a very fine pipette, identified from life using a magnification of 200–400× and then impregnated (note that it is usual to use only few specimens with the modification of the silver carbonate method described in [21]). *Metopus* spp. are not particularly difficult to impregnate with this method, especially those species which have inconspicuous cortical granules (mucocysts).

Counts and measurements on randomly selected, protargol-impregnated and mounted morphostatic specimens were performed at a magnification of 1,000×. In vivo measurements were made at magnifications of 40–1,000×. While the latter measurements provide only rough estimates, it is worth giving such data as specimens usually shrink in preparations. Statistics were calculated according to textbooks. Illustrations of live specimens were based on free-hand sketches, micrographs and video records; those of impregnated cells were made with a camera lucida. All figures were orientated with the anterior end of the organism directed to the top of the page. Terminology is mainly according to Jankowski [31]; the somatic ciliary rows extending dorsally onto the preoral dome are named "dome kineties", the first being nearest to the perizonal ciliary stripe, whose kineties are numbered from the posterior to the anterior dome margin (Fig. 6).

## RESULTS

Morphometric data shown in Table 1 are repeated in this section only as needed for clarity and are based on material obtained with the non-flooded Petri dish method.

### *Metopus hasei* Sondheim, 1929
(Fig. 1–26 and Table 1)

**Synonymy.** Several populations of *M. hasei* have been studied [12, 19, 46]. They are very similar and match the Namibian and South African specimens well, at least as concerns the main characteristics, namely, shape of body and adoral zone of membranelles, location of nuclear apparatus, caudal cilia, and cortical granulation; most morphometric features show strong interpopulation variability, indicating microspecies formation. The improved diagnosis given below summarizes the data available, including the very detailed results from the populations of Namibia and South Africa as well as occasional observations from other strains worldwide. Esteban et al. [15] synonymized *M. latusculisetus* Tucolesco, 1962 [49] and *M. fusus* Vuxanovici, 1962 [52] with *M. hasei*; this seems justified at the present state of knowledge.

**Improved diagnosis.** Size in vivo usually 80–130 × 15–30 μm. Overall shape cylindroidal; preoral dome slender and indistinctly projecting above ventral surface, inclined about 45° to main body axis projecting distinctly above left body margin. Macronucleus ellipsoidal and usually in anterior body half left of adoral zone of membranelles. Cortical granules inconspicuous. Five perizonal and usually 10–15 somatic ciliary rows, of which two to three extend onto preoral dome. About five distinctly elongated caudal cilia. Adoral zone occupies circa 35–45% of body length on average, terminates on ventral side right of midline slightly underneath perizonal stripe, composed of about 16–24 membranelles.

**Description.** Size in vivo 70–90 × 17–24 μm [46], 70–100 × 13–18 μm [19] and 80–90 μm [12], occasionally up to 118 × 35 μm [46]; protargol-impregnated specimens (n = 6) 57–75 × 12–19 μm [19] and 51 × 13 μm (n = 6) on average [12], which matches the Namibian population very well (43–89 × 16–29 μm, Table 1) and is considerably smaller than the South African specimens (92–129 × 14–30 μm, Table 1). Overall shape cylindroidal, length:width ratio highly variable within and between populations both in vivo and protargol slides, where *M. hasei* is considerably stouter than when alive: in vivo 2.5–6:1, usually 4:1–5:1; after protargol impregnation 1.8:1–7.6:1, usually 2.7:1–4.9:1 (Table 1 and Fig. 23, 24). Ratio of preoral:postoral body portion also rather variable, usually about 1:1–1:1.9 (Table 1). Preoral dome only slightly sigmoidal, distinctly curved and inclined about 45° to main body axis, projecting knob-like above anterior left body margin; inconspicuous because without distinct brim, narrow, dorsoventrally flattened about 2:1, and hardly projecting above ventral surface merging smoothly into right side in middle third of cell (Fig. 1–4, 8–11, 16–19, 25, 26). Postoral body portion cylindroidal with rear end slightly narrowed and evenly rounded, frequently with more or less distinct folds, especially after systole of contractile vacuole (Fig. 1, 13). Macronucleus typically in anterior body half left of adoral zone of membranelles, in vivo about 28–36 × 8–14 μm, that is, short to long-ellipsoidal, ovoidal or reniform, length:width ratio usually about 2–4.5:1 (Table 1); contains numerous nucleoli 0.6–1.5 μm across. Micronucleus usually near or attached to anterior third of macronucleus, globular to ellipsoidal, surrounded by distinct membrane in alpine population (Fig. 5). Contractile vacuole in posterior end, with very short canal extending to argyrophilic cytopyge slit on posterior pole (Fig. 3), indicating that a separate excretory pore is lacking, as in *M. inversus*. Cortex flexible, slightly furrowed by ciliary rows, contains colourless granules difficult to recognize in vivo but occasionally distinct in protargol and methyl green-pyronin preparations, being rather densely arranged and 0.2–0.7 μm across (Fig. 14); tightly underneath cortex pale, ellipsoidal granules, possibly hydrogenosomes. Cytoplasm colourless, hyaline, especially in posterior body portion, bacterial rods, probably methanogens, impregnate with protargol and/or silver carbonate in some populations. Food vacuoles 4–14 μm across, contain bacteria (Fig. 2, 12). Movement moderately fast by rotation about main body axis.

Normal somatic cilia 10 μm long, those of perizonal stripe and underneath buccal vertex elongated to 13 μm. Invariably about four to six caudal cilia, whose length varies considerably in different populations: as long as body [46], about 30 μm [19], 35 μm in live specimens from a riparian forest soil in Lower Austria, 30–45 μm ($\bar{x}$ = 38.8 μm, n = 10) in protargol-impregnated cells from Namibia, and 30–76 μm ($\bar{x}$ = 50 μm, n = 19) in protargol-impregnated specimens from South Africa. Number of ciliary rows rather variable, about 15 in type population (as estimated from Fig. 1) and in Namibian and South African specimens (Table 1), only 10 in the alpine population from Austria (Table 1). Ciliary rows slightly shortened posteriorly, leaving blank a small, roughly circular area containing the cytopyge, every second to third row elongated by one dikinetid bearing a caudal cilium; composed of dikinetids orientated parallel to slightly obliquely to kinety axis and having only the posterior basal body ciliated, except the anterior portion of the dome and postcytostomial [19] kineties and the whole perizonal ciliary rows, where both basal bodies are ciliferous; longitudinally and equidistantly arranged in Namibian and South African specimens, slightly narrower spaced dorsally than ventrally in Austrian population, where often a rather distinct glabrous stripe occurs in midline. Postoral (ventral) kineties distinctly separate from adoral zone of membranelles, dorsal kineties anteriorly shortened from right to left. Two dome kineties in Austrian, three in Namibian and South African specimens, each composed of about 18–30 dikinetids. Perizonal stripe slightly shorter than adoral zone of membranelles (about 35% of body length, Table 1), about 2–3 μm wide, composed of five narrowly spaced kineties following curvature of dome margin; kineties 4 and 5 slightly shortened anteriorly and posteriorly and slightly apart from and more widely spaced than

Table 1. Morphometric data from three populations (Pop) of *Metopus hasei* (MA, Austria[a]; MN, Namibia; MS, South Africa) and one population of *Metopus inversus* (MI).

| Character[b] | Pop | $\bar{x}$ | M | SD | SE | CV | Min | Max | n |
|---|---|---|---|---|---|---|---|---|---|
| Body, length | MN | 60.1 | 59.0 | 9.1 | 2.08 | 15.1 | 43.0 | 89.0 | 19 |
| | MS | 113.4 | 113.0 | 7.4 | 1.71 | 6.6 | 92.0 | 129.0 | 19 |
| | MA | 65.5 | 63.5 | 7.2 | 2.94 | 11.0 | 57.0 | 75.0 | 6 |
| | MI | 75.0 | 73.0 | 8.2 | 1.88 | 10.9 | 63.0 | 91.0 | 19 |
| Body, total width[d] | MN | 21.1 | 20.0 | 3.4 | 0.73 | 15.9 | 16.0 | 29.0 | 19 |
| | MS | 23.6 | 24.0 | 4.1 | 0.95 | 17.6 | 14.0 | 30.0 | 19 |
| | MI | 47.0 | 48.0 | 5.4 | 0.79 | 11.5 | 38.0 | 61.0 | 19 |
| Body, width at cytostome | MN | 15.2 | 15.0 | 1.3 | 0.29 | 8.3 | 13.0 | 18.0 | 19 |
| | MS | 14.5 | 14.0 | 1.9 | 0.43 | 12.8 | 11.0 | 18.0 | 19 |
| | MA | 9.5 | 9.0 | 1.8 | 0.72 | 18.5 | 8.0 | 12.0 | 6 |
| | MI | 37.8 | 38.0 | 5.4 | 1.23 | 14.2 | 29.0 | 45.0 | 19 |
| Body, maximum postoral width | MN | 17.7 | 18.0 | 1.6 | 0.37 | 9.2 | 15.0 | 20.0 | 19 |
| | MS | 21.3 | 22.0 | 3.0 | 0.68 | 14.0 | 14.0 | 25.0 | 19 |
| | MA | 15.3 | 16.0 | 2.5 | 1.02 | 16.3 | 12.0 | 19.0 | 6 |
| | MI | 37.8 | 38.0 | 5.4 | 1.23 | 14.2 | 29.0 | 45.0 | 19 |
| Body, length : total width, ratio[d] | MN | 2.8 | 2.8 | 0.5 | 0.30 | 17.6 | 1.8 | 3.6 | 19 |
| | MS | 4.9 | 4.9 | 0.8 | 0.19 | 17.2 | 3.8 | 7.6 | 19 |
| | MI | 1.7 | 1.8 | 0.3 | 0.23 | 17.2 | 1.2 | 2.3 | 19 |
| Anterior cell end to posterior end of perizonal stripe, distance | MN | 20.6 | 21.0 | 2.7 | 0.60 | 12.9 | 14.0 | 25.0 | 19 |
| | MS | 37.6 | 38.0 | 2.9 | 0.67 | 7.7 | 33.0 | 45.0 | 19 |
| | MI | 48.9 | 48.0 | 5.5 | 1.27 | 11.3 | 39.0 | 61.0 | 19 |
| Anterior cell end to proximal end of adoral zone of membranelles, distance | MN | 23.2 | 24.0 | 1.9 | 0.40 | 8.1 | 19.0 | 25.0 | 19 |
| | MS | 49.3 | 50.0 | 2.7 | 0.63 | 5.5 | 45.0 | 56.0 | 19 |
| | MA | 22.0 | 23.0 | 3.0 | 1.21 | 13.5 | 17.0 | 25.0 | 6 |
| | MI | 39.1 | 38.0 | 5.2 | 1.19 | 13.3 | 31.0 | 48.0 | 19 |
| Distance anterior end to end of perizonal stripe : body length, ratio in % | MN | 35.4 | 35.9 | 4.7 | 1.07 | 13.2 | 25.9 | 43.1 | 19 |
| | MS | 33.2 | 33.9 | 2.2 | 0.50 | 6.6 | 28.8 | 35.9 | 19 |
| | MI | 63.5 | 66.3 | 7.7 | 1.78 | 12.2 | 52.3 | 73.8 | 19 |
| Distance anterior end to end of adoral zone of membranelles : body length, ratio in % | MN | 39.8 | 39.7 | 2.6 | 0.59 | 6.4 | 36.5 | 45.1 | 19 |
| | MS | 43.6 | 43.4 | 2.6 | 0.60 | 6.0 | 40.2 | 52.2 | 19 |
| | MA | 33.6 | 33.1 | 3.0 | 1.21 | 8.8 | 29.8 | 37.7 | 6 |
| | MI | 48.7 | 47.9 | 4.1 | 0.94 | 8.4 | 42.9 | 55.8 | 19 |
| Macronucleus, length | MN | 18.8 | 18.0 | 2.9 | 0.66 | 15.4 | 14.0 | 26.0 | 19 |
| | MS | 36.7 | 38.0 | 5.4 | 1.25 | 14.8 | 26.0 | 45.0 | 19 |
| | MA | 17.3 | 16.5 | 3.0 | 1.23 | 17.4 | 15.0 | 23.0 | 6 |
| | MI | 28.8 | 29.0 | 3.9 | 0.89 | 13.5 | 19.0 | 35.0 | 19 |
| Macronucleus, width | MN | 8.8 | 9.0 | 0.8 | 0.18 | 9.0 | 8.0 | 10.0 | 19 |
| | MS | 7.9 | 8.0 | 2.0 | 0.45 | 24.6 | 4.0 | 12.0 | 19 |
| | MA | 7.8 | 8.0 | 0.7 | 0.31 | 9.6 | 7.0 | 9.0 | 6 |
| | MI | 11.1 | 10.0 | 2.5 | 0.58 | 22.7 | 8.0 | 15.0 | 19 |
| Anterior cell end to posterior end of macronucleus, distance | MN | 30.1 | 30.0 | 3.9 | 0.90 | 13.1 | 23.0 | 41.0 | 19 |
| | MS | 62.4 | 61.0 | 13.9 | 3.18 | 22.2 | 44.0 | 87.0 | 19 |
| | MA | 35.7 | 34.0 | 6.2 | 2.55 | 17.5 | 29.0 | 45.0 | 6 |
| | MI | 23.2 | 23.0 | 3.4 | 0.78 | 14.7 | 16.0 | 30.0 | 19 |
| Micronucleus, length | MN | 3.9 | 4.0 | 0.7 | 0.17 | 18.9 | 3.0 | 6.0 | 19 |
| | MS | 3.0 | 3.0 | 0.2 | 0.05 | 7.5 | 3.0 | 4.0 | 19 |
| | MA | 3.0 | 2.9 | 0.4 | 0.16 | 13.5 | 2.6 | 3.7 | 6 |
| | MI | 5.3 | 5.0 | 1.1 | 0.24 | 19.9 | 4.0 | 8.0 | 19 |
| Micronucleus, width | MN | 3.3 | 3.0 | 0.6 | 0.13 | 17.2 | 3.0 | 5.0 | 19 |
| | MS | 2.7 | 3.0 | 0.6 | 0.13 | 21.7 | 2.0 | 4.0 | 19 |
| | MA | 3.0 | 2.9 | 0.4 | 0.16 | 13.5 | 2.6 | 3.7 | 6 |
| | MI | 4.5 | 4.0 | 1.0 | 0.22 | 21.3 | 4.0 | 8.0 | 19 |
| Macronucleus, number | MN | 1.0 | 1.0 | 0.0 | 0.00 | 0.0 | 1.0 | 1.0 | 19 |
| | MS | 1.0 | 1.0 | 0.0 | 0.00 | 0.0 | 1.0 | 1.0 | 19 |
| | MA | 1.0 | 1.0 | 0.0 | 0.00 | 0.0 | 1.0 | 1.0 | 6 |
| | MI | 1.0 | 1.0 | 0.0 | 0.00 | 0.0 | 1.0 | 1.0 | 19 |
| Micronucleus, number | MN | 1.0 | 1.0 | 0.0 | 0.00 | 0.0 | 1.0 | 1.0 | 19 |
| | MS | 1.0 | 1.0 | 0.0 | 0.00 | 0.0 | 1.0 | 1.0 | 19 |
| | MA | 1.0 | 1.0 | 0.0 | 0.00 | 0.0 | 1.0 | 1.0 | 6 |
| | MI | 1.0 | 1.0 | 0.0 | 0.00 | 0.0 | 1.0 | 1.0 | 19 |
| Somatic ciliary rows, number | MN | 14.6 | 15.0 | 1.5 | 0.34 | 10.0 | 10.0 | 16.0 | 19 |
| | MS | 14.6 | 14.0 | 0.7 | 0.16 | 4.7 | 14.0 | 16.0 | 19 |
| | MA | 10.0 | 10.0 | 0.0 | 0.00 | 0.0 | 10.0 | 10.0 | 6 |
| | MI | 23.7 | 24.0 | 1.2 | 0.28 | 5.2 | 22.0 | 25.0 | 19 |

(Continued)

Table 1. Continued.

| Character[b] | Pop | $\bar{x}$ | M | SD | SE | CV | Min | Max | n |
|---|---|---|---|---|---|---|---|---|---|
| Caudal cilia, number | MN | 5.0 | 5.0 | 0.4 | 0.18 | 8.0 | 4.0 | 6.0 | 19 |
| | MS | 5.0 | 5.0 | 0.4 | 0.10 | 7.8 | 4.0 | 6.0 | 19 |
| Adoral membranelles, number | MN | 16.4 | 16.0 | 1.0 | 0.22 | 5.8 | 15.0 | 18.0 | 19 |
| | MS | 23.6 | 24.0 | 1.3 | 0.31 | 5.7 | 21.0 | 26.0 | 19 |
| | MA | 18.5 | 18.0 | 1.2 | 0.50 | 6.6 | 17.0 | 20.0 | 6 |
| | MI | 33.3 | 33.0 | 1.8 | 0.42 | 5.5 | 29.0 | 37.0 | 19 |
| Perizonal ciliary rows, number | MN | 5.0 | 5.0 | 0.0 | 0.00 | 0.0 | 5.0 | 5.0 | 19 |
| | MS | 5.0 | 5.0 | 0.0 | 0.00 | 0.0 | 5.0 | 5.0 | 19 |
| | MA | 5.0 | 5.0 | 0.0 | 0.00 | 0.0 | 5.0 | 5.0 | 6 |
| | MI | 5.0 | 5.0 | 0.0 | 0.00 | 0.0 | 5.0 | 5.0 | 19 |
| Perizonal ciliary rows, number of "false" kineties[c] | MN | 24.9 | 25.0 | 1.7 | 0.38 | 6.7 | 20.0 | 28.0 | 19 |
| | MS | 31.5 | 31.0 | 2.2 | 0.51 | 7.0 | 28.0 | 36.0 | 19 |
| | MA | 24.7 | 25.0 | 0.8 | 0.33 | 3.3 | 23.0 | 25.0 | 6 |
| | MI | 63.0 | 65.0 | 4.7 | 1.07 | 7.2 | 58.0 | 74.0 | 19 |

[a] Recalculated from raw data of Austrian population studied by [19].
[b] Data based on protargol-impregnated, mounted specimens from non-flooded Petri dish cultures. Measurements in μm. CV, coefficient of variation in %; M, median; Max, maximum; Min, minimum; n, number of individuals investigated; SD, standard deviation: SE, standard error of arithmetic mean; $\bar{x}$, arithmetic mean.
[c] See description of species.
[d] Total width = including projecting anterior portion of preoral dome. Cells were not selected for a particular orientation.

kineties 1–3 (Fig. 3, 6). Perizonal dikinetids widely spaced, those of rows 1–3 form 20–36 (Table 1) short, straight ("false") kineties alternately arranged to dikinetids of kineties 4 and 5, producing arrow-like pattern (Fig. 3, 6; these kineties are recognizable, although less clearly, also in previous illustrations, Fig. 2, 5, 8).

Somatic dikinetids associated with four conspicuous structures after silver carbonate impregnation (Fig. 7, 20–22; see also *M. inversus,* Fig. 44, 45, 48–50; a very similar pattern is recognizable, albeit less clearly, after protargol impregnation, especially in *M. gibbus,* unpubl. observ.; see Discussion for interpretation, here they are designated as "structures a, b, c, d"): anterior basal body associated with structure (a) directed to the left and slightly anteriad; posterior basal body associated with structure (c) extending obliquely posteriad, an anterolaterally-directed structure (d) on the right, and a structure (b) extending to the left and very slightly posteriad, forming an acute angle with structure (a) of the anterior basal body. The length of the associates depends on the body region and is especially diverse in the perizonal ciliary stripe, producing its peculiar texture after silver carbonate impregnation. Structures (a, b) are distinctly longer than structure (c), both are very short in the perizonal stripe, except for structure (c) in row 1, which extends between the "false" kineties. Structure (d) is about as long as structure (c) in the postoral body portion, its length distinctly increases anteriad in the dome kineties and, especially, in the mid-ventral portion of perizonal ciliary row 5 (Fig. 20, 21).

Adoral zone of membranelles slightly sigmoidal, hardly roofed by preoral dome, commences at anterior left margin of preoral dome and extends obliquely to right body margin, performing a slight clockwise rotation when plunging into the shallow buccal cavity slightly above mid-body (Fig. 2, 3, 5, 18, 19, 23–26); consists of 17–20 membranelles in Austrian, 15–18 in Namibian, and 21–26 in South African population (Table 1). Zone composed of a long distal and a very short proximal portion distinctly different in the structure of the membranelles (Fig. 15): distal membranelles cuneiform because composed of two long (2–3 μm) rows of zigzagging basal bodies to which a short row is attached at right anterior end; proximal (buccal) membranelles rectangular and composed of only two rows of basal bodies. Paroral membrane in corner formed by preoral dome and ventral surface, short and almost straight, extends to proximal end of buccal cavity, composed of basal bodies in single line bearing about 10-μm-long cilia, appears rather thick in silver slides due to adhering (pharyngeal) fibres, which form dorsally directed funnel extending to near posterior body end (Fig. 3, 5, 15, 20, 26).

**Occurrence and ecology.** Sondheim [46] discovered *M. hasei* in rewetted mud from an unknown locality in Madagascar, and the population developed best in old infusions covered with a thick layer of *Oscillatoria. Metopus hasei* has since been found in terrestrial habitats from all main biogeographical regions except Antarctica [6, 19, 23, 25]; it has also been reliably recorded from the sapropel of a lake in Romania [53]. In our experience, *M. hasei* is indicative for soils which are at least occasionally microaerobic or anaerobic. In the laboratory, usually it develops only in old cultures with microaerobic or anaerobic microsites.

**Comparison with related species.** *Metopus hasei* is similar to *M. palaeformis* Kahl, 1927 [33] in shape, size, and number of ciliary rows (8–14) and adoral membranelles (10–20). Unfortunately, Esteban et al. [15] did not provide details of the infraciliature of *M. palaeformis.* In spite of this, *M. hasei* and *M. palaeformis* can be easily separated because the latter lacks caudal cilia [15, 33, 34]. The South African specimens of *M. hasei* are very similar to *M. laminarius* f. *minor* Kahl, 1932 [34], indicating synonymy. However, a reliable comparison is impossible because the infraciliature of both *M. laminarius* (length 200–250 μm) and *M. laminarius* f. *minor* (150 μm) is not known.

*Metopus inversus* (Jankowski, 1964) nov. comb.
(Fig. 27–53, Table 1)

**Improved diagnosis.** Size in vivo about 80 × 50 μm. Mushroom-shaped due to laterally and ventrally widely projecting preoral dome and narrowed, ellipsoidal postoral body portion. Dome conspicuously sigmoidal and flattened, contains reniform macronucleus. Cortical granules inconspicuous. Five perizonal and 24 somatic ciliary rows on average, of which 4 extend onto preoral dome. Adoral zone slightly shorter than perizonal stripe,

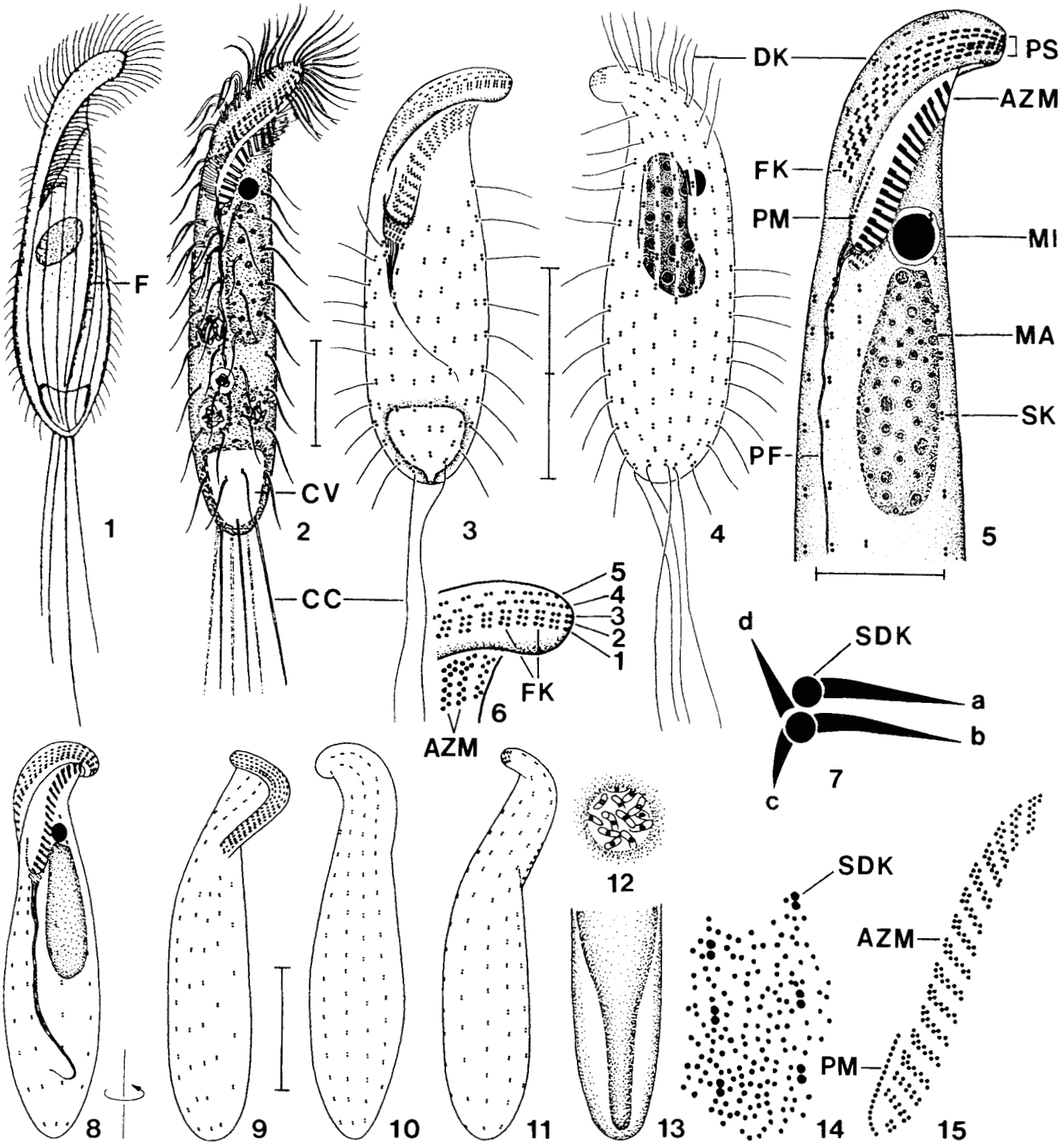


Fig. 1–15. *Metopus hasei* from life (1, 2, 12, 13) and after protargol (3–6, 8–11, 14, 15) and silver carbonate (7) impregnation. Madagascan-type population: Fig. 1 [from 46]; Namibian population: Fig. 3, 4, 6, 7, 14, 15; Austrian population: Fig. 2, 5, 8–13 [from 19]. **1, 2.** Ventral view of representative specimens, length 70–100 μm. **3, 4.** Infraciliature of ventral and dorsal side. **5, 6.** Details of anterior ventral side. **7.** Structures associated with a somatic dikinetid after silver carbonate impregnation (for details, see Discussion and Fig. 83–85). **8–11.** Main aspects of body shape and ciliature during counterclockwise rotation about main body axis: ventral (8), right lateral (9), dorsal (10), left lateral (11). **12.** Food vacuole with bacteria. **13.** Rear end after systole of contractile vacuole. **14.** Cortical granulation. **15.** Oral structures. Membranelle structure is different in the long distal and the short proximal portion of the adoral zone. a–d, structures associated with a somatic dikinetid; AZM, adoral zone of membranelles; CC, caudal cilia; CV, contractile vacuole; DK, dome kineties; F, fold; FK, "false" kineties formed by perizonal rows 1–3; MA, macronucleus; MI, micronucleus; PF, pharyngeal fibres; PM, paroral membrane; PS, perizonal stripe; SDK, somatic dikinetid; SK, somatic kinety; 1–5, perizonal ciliary rows. Bar division = 20 μm (Fig. 2–4, 8–11) and 10 μm (Fig. 5).

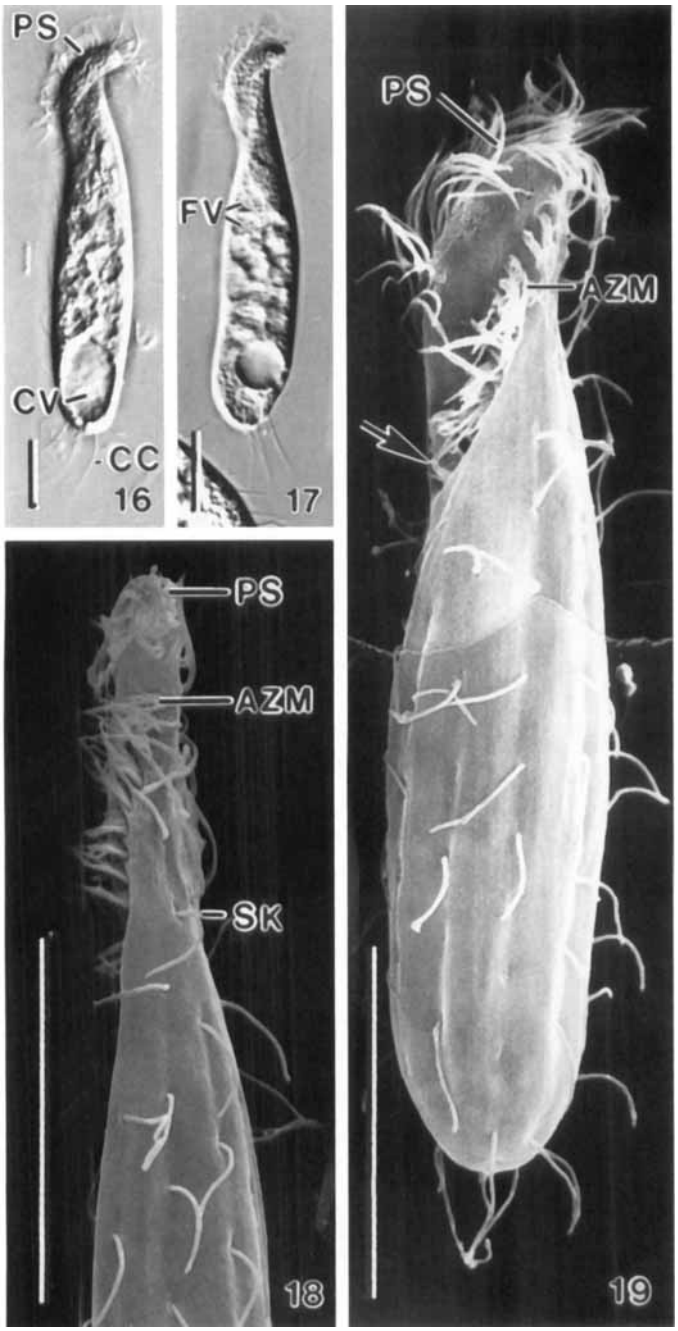


Fig. **16–19**. *Metopus hasei*, Venezuelan specimens in vivo (16, 17) and in the scanning electron microscope (18, 19). **16**, **17**. Ventral and ventrolateral view showing the typical body shape, the elongated caudal cilia, and the preoral dome, which is inclined about 45° and projects distinctly above left body margin. **18**. Anterior portion of left side showing anterior end of adoral zone of membranelles and narrow, dorsoventrally flattened preoral dome hardly projecting above ventral surface. **19**. Ventrolateral view showing the inconspicuous preoral dome, which hardly covers the slightly sigmoidal adoral zone of membranelles; the zone commences at the anterior left margin and extends obliquely to the right margin, where it plunges into the shallow buccal cavity (arrow). Caudal cilia shrunk due to preparation procedures. AZM, adoral zone of membranelles; CC, caudal cilia; CV, contractile vacuole; FV, food vacuoles; PS, perizonal ciliary stripe; SK, somatic kinety. Bars = 20 μm.

terminates in mid-body on right margin of cell, composed of 33 adoral membranelles on average.

**Neotype material.** No type material of *M. inversus* has been mentioned in the literature. Thus, we deposit 6 neotype slides with protargol-impregnated morphostatic and dividing cells from the Aubschlucht in Namibia, Southwest Africa (16° 20′ E, 24° S), in the Oberösterreichische Landesmuseum in Linz (LI). The slides contain many specimens, with relevant cells marked by a black ink circle on the cover glass.

**Description of Namibian population.** Size in vivo 70–100 × 40–70 μm, usually about 80 × 50 μm, as calculated from some measurements of live specimens and values shown in Table 1; length:width ratio highly variable (1.2–2.3:1), usually 1.7:1, ratio of preoral:postoral body portion also rather variable, on average about 1:1 (Table 1). Overall shape mushroom-like, it depends, however, on the side viewed due to the widely overhanging and sigmoidally ascending preoral dome occupying about one fifth of body length in ventral view (Fig. 34–40). Preoral dome, although thin and hyaline, very conspicuous because widely projecting above ventral and lateral body surface, extends almost perpendicularly above ventral side and merges into body proper slightly underneath mid-body on right margin of dorsal side (Fig. 35–40); central dome portion slightly convex, broadly sigmoidal in top view due to curved dome brim, which forms sharp corner with dorsal side anteriorly (Fig. 29, 46, 47). Postoral body portion (mushroom stem) ellipsoidal with ventral and left side more distinctly convex than right and dorsal, causing a slight, sigmoidal torsion of the organisms, described rather cryptically by Jankowski as "sigmoid body with double winding". Rear third of body with some more or less pronounced folds after systole of contractile vacuole. Macronucleus invariably in preoral dome, reniform, contains numerous nucleoli. Micronucleus ellipsoidal, usually near or attached to ventral anterior end of macronucleus. Cytopyge subterminal on ventral side, slit-like (Fig. 33, 41, 53), very likely also functioning as discharge device for the contractile vacuole because no excretory pore could be found. Cortex slightly furrowed by ciliary rows, contains inconspicuous, loosely arranged, colourless granules 0.2–0.5 μm across (Fig. 30), which stain red with methyl green-pyronin. Cytoplasmic bacteria neither recognizable in vivo nor after silver carbonate and protargol impregnation (where they stained well in *M. gibbus* contained in the same slides); no particular accumulation of granules in preoral dome. Food vacuoles 5–15 μm across, contained bacteria and their spores (Fig. 29). Movement moderately fast, without peculiarities.

Somatic cilia about 15 μm long in vivo, lack of elongated caudal cilia checked in live and over-impregnated specimens. Ciliary rows composed of dikinetids orientated parallel to slightly obliquely to kinety axis and having only the posterior basal body ciliated, except perizonal ciliary rows and anterior portion of dome kineties, where both basal bodies are ciliferous (Fig. 29, 41); longitudinally and equidistantly arranged underneath membranellar zone, dorsally distances increase from right to left. Postoral (ventral) kineties distinctly separate from adoral zone of membranelles, slightly shortened posteriorly, leaving blank a small, roughly circular area containing the cytopyge (Fig. 33, 53). Dorsal kineties anteriorly shortened from right to left, while slightly elongated posteriorly and thus extending across pole to circular patch containing the cytopyge. Accordingly, the posterior cell pole does not entirely coincide with the kinety pole, which is subterminally on the ventral side. Ciliary pattern rather irregular underneath buccal vertex and at posterior end of perizonal stripe, where some scattered dikinetids occur (Fig. 41, 48). Three to four dome kineties, number 1 as long as perizonal stripe, numbers 2–4 slightly shortened ante-

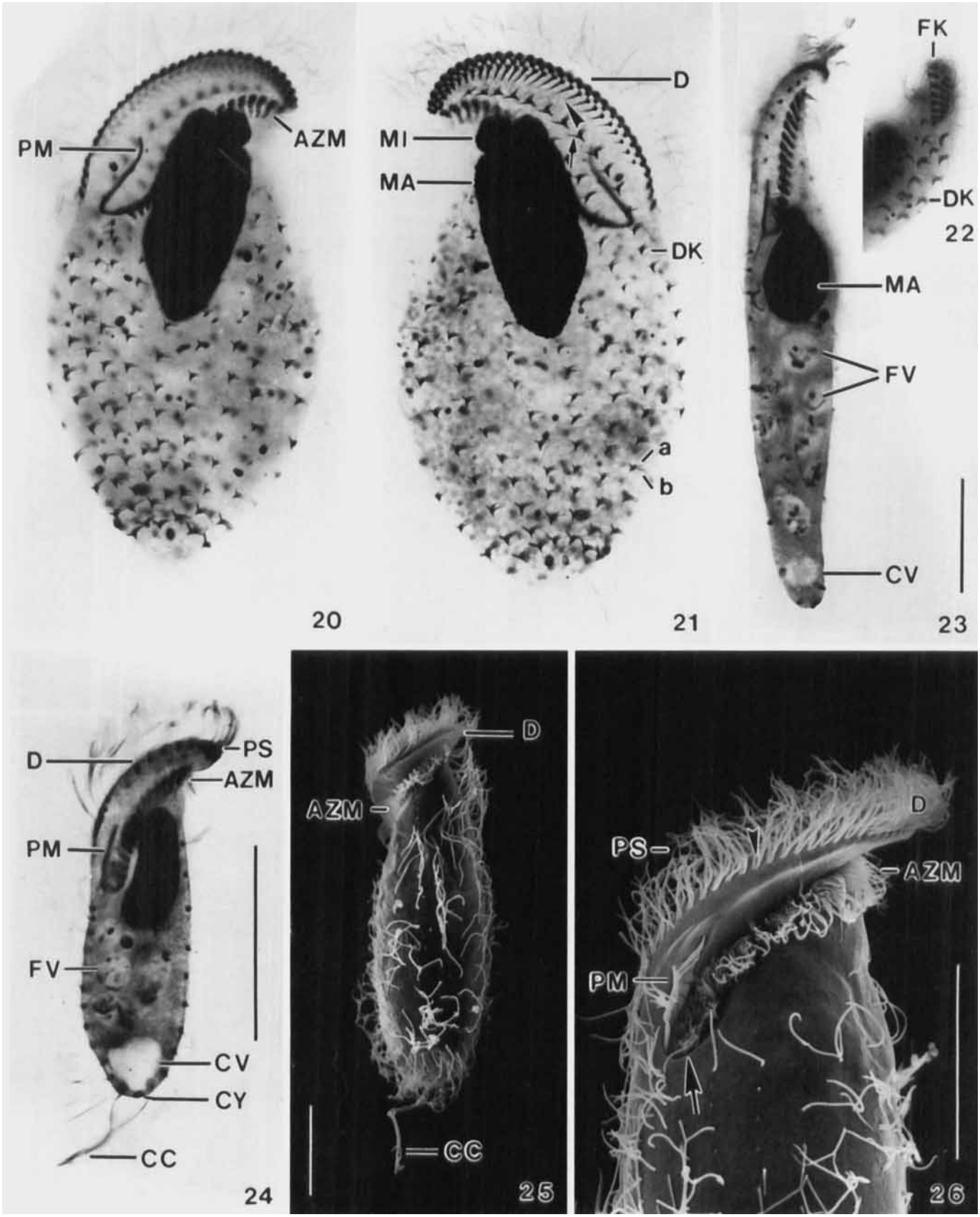


Fig. **20–26**. *Metopus hasei*, Namibian specimens after silver carbonate (20–22) and protargol (23, 24) impregnation, and Austrian specimens in the scanning electron microscope (25, 26). **20, 21**. Infraciliature of ventral and dorsal side of same specimen. The cell was heavily squashed

riorly and extending to posterior body end; distances between dome kineties decrease from ventral to dorsal (Fig. 47, 52). Perizonal ciliary stripe slightly longer than adoral zone of membranelles (about 65% of body length, Table 1), about 3 μm wide, composed of five very narrowly spaced kineties following curvature of dome margin, kineties 4 and 5 slightly shortened anteriorly and posteriorly and slightly apart from and more widely spaced than kineties 1–3. Perizonal dikinetids widely spaced, those of rows 1–3 form 58–74 short, straight ("false") kineties alternately arranged to dikinetids of kineties 4 and 5, producing arrow-like pattern (Table 1 and Fig. 41, 45, 49).

The associates of the somatic dikinetids and their orientation match those of *M. hasei* (cp. Fig. 7, 20, 21 with Fig. 44, 48, 52). Likewise, the length of the associates depends on the body region and is especially diverse in the kinetids of the perizonal stripe, producing its peculiar texture after silver carbonate impregnation (Fig. 45, 49, 50). Structures (a, b, c) are longest in the posterior half of the postcytostomial ciliary rows and in the anterior half of the dorsal and dome kineties, except the anteriormost one to two dikinetids (Fig. 48, 52). Structure (d) is elongated in the anterior dome area, increasing in length from posterior to anterior and from dorsal to ventral and, especially, in the mid-ventral portion of perizonal ciliary row 5 (Fig. 45, 49, 50). In the perizonal ciliary rows most associates are short (Fig. 45, 49), except structure (d) of row 5, as described above; structure (a) of rows 2 and 5; structures (a, b) of row 4, which extend to row 3 and diverge so strongly that each touches one of the short, "false" kineties; and structure (c) of row 1, which extends between the short "false" kineties.

Adoral zone of membranelles sigmoidal, entirely roofed by dome brim, commences at anterior dorsal end of preoral dome and extends obliquely to mid-body and right side, where it plunges into the short buccal cavity performing a slight clockwise rotation (Fig. 29, 41, 42, 50, 51). Zone composed of a long distal and a short proximal portion which differ distinctly in the structure of the membranelles (Fig. 43, 51): distal membranelles cuneiform because composed of two, about 3 μm long rows of zigzagging basal bodies to which a short row is attached at right anterior end; proximal (buccal) membranelles rectangular and composed of four rows of basal bodies, those in mid of buccal cavity slightly longer (about 5 μm) than all other membranelles. Paroral membrane in corner formed by preoral dome and ventral surface, commences near midline of cell and curves to proximal end of buccal cavity, composed of ciliated basal bodies in single line, appears rather thick in silver slides due to adhering (pharyngeal) fibres, which form long, dorsally directed funnel with fibres widely spaced in aperture region (Fig. 41, 48, 50).

**Occurrence and ecology.** *Metopus inversus* was discovered in ponds near Leningrad [31]. Our record is the first from soil. However, the sample was taken from the margin of a pool communicating with a nearby stream; very likely, this area becomes inundated during floods of the stream. Thus, resting cysts of *M. inversus* may have been deposited by chance in the surface layer of the soil. On the other hand, *M. inversus* reproduced in our soil culture, which shows that it is able to live in this biotope. Whether *M. inversus* really lacks cytoplasmic bacteria, as indicated by the observations mentioned above, needs more detailed investigations.

**Comparison with original description and related species.** Metopids have a complicated shape and thus many different aspects (Fig. 35–40). We identified our population as *Brachonella inversa* because the two (uncommon) views Jankowski [30] showed almost perfectly match some of our illustrations, and both populations have the macronucleus in the preoral dome and lack caudal cilia (cp. Fig. 27 with 39, 46 and Fig. 28 with 38). Furthermore, the size of preserved specimens (63–91 × 38–61 μm vs. 90–105 × 51 μm) and the long perizonal stripe agree with Jankowski's description. However, there are also some (minor) differences, namely the perizonal stripe, which is slightly shorter than the adoral zone of membranelles in our population, and the dome brim, whose hook-like dorsolateral projection was not described by Jankowski. Both characters are difficult to recognize without video microscopy and silver impregnation. Thus, it is reasonable to assume that he overlooked them.

In vivo, *B. inversa* looks like a stoutish *Metopus hasei*. However, both are easily distinguished by the location of the macronucleus (in preoral dome vs. postoral body portion) and the caudal cilia (lacking vs. present). In silver preparations, they differ by the number of somatic kineties (22–25 vs. 10–16).

The identification of metopids is difficult [15, 34], mainly because very few species have been thoroughly studied and no type material is available. This is also evident from the debates above and below. Thus, we fix our specimens of *M. inversus* from Namibia as neotype, although they are not from the type locality (region), as they should be (article 75d(5) of [29]).

**Generic classification.** Jankowski [30, 31] split *Metopus* into several genera and subgenera. *Brachonella* differs from *Metopus* mainly by the subterminal, dorsal location of the cytostome due to the strongly spiralized adoral zone of membranelles. Jankowski's figures of *B. inversa* largely agree with our observations and show that the adoral zone of membranelles hardly extends onto the dorsal side and certainly not to the posterior body end (Fig. 27, 28). This contradicts his description, at least partially, which is based on unstained, mercuric chloride preserved specimens: "The elongated adoral zone of membranelles makes a spiralling band, that shifts the cytostome on the dorsal body surface to the posterior end. This spiral is much longer in *B. spiralis*; in this respect, *B. inversa* occupies an intermediate position between *Metopus es* and *Brachonella spiralis*". According to our investigations, *B. inversa* is a typical member of *Metopus* (*Metopus*) because the cytostome is near mid-body (Jankowski did not recognize that the adoral zone is slightly shorter than the perizonal stripe; see discussion of species above) and in the transition zone of the right and dorsal side. Accordingly, we combine *Brachonella* (*Brachonella*) *inversa* Jankowski, 1964 to *Metopus* (*Metopus*) *inversus*

←

(thus without scale bar) to show as many details as possible. The length of the structures associated with the somatic dikinetids (cp. Fig. 7) increases anteriad in the dome kineties (arrow) and, especially, in perizonal row 5 (arrowhead). **22.** Anterior end of dome kineties and perizonal stripe, rows 1–3 which form short, "false" kineties. **23, 24.** Ventral view of a slender and a stout specimen, both with numerous food vacuoles. **25.** Ventrolateral view showing preoral dome hardly projecting above ventral side. **26.** Ventral view of anterior cell portion showing preoral dome widely projecting above left body margin and slightly sigmoidal adoral zone of membranelles plunging into buccal cavity (arrow). Note that both basal bodies of the dikinetids are ciliated (arrowhead) in the perizonal rows. a, b, structures associated with the somatic dikinetids (cp. Fig. 7); AZM, adoral zone of membranelles; CC, caudal cilia; CV, contractile vacuole; CY, cytopyge; D, preoral dome; DK, dome kineties; FK, "false" kineties formed by perizonal rows 1–3; FV, food vacuoles; MA, macronucleus; MI, micronucleus; PM, paroral membrane; PS, perizonal ciliary stripe. Bars = 20 μm.

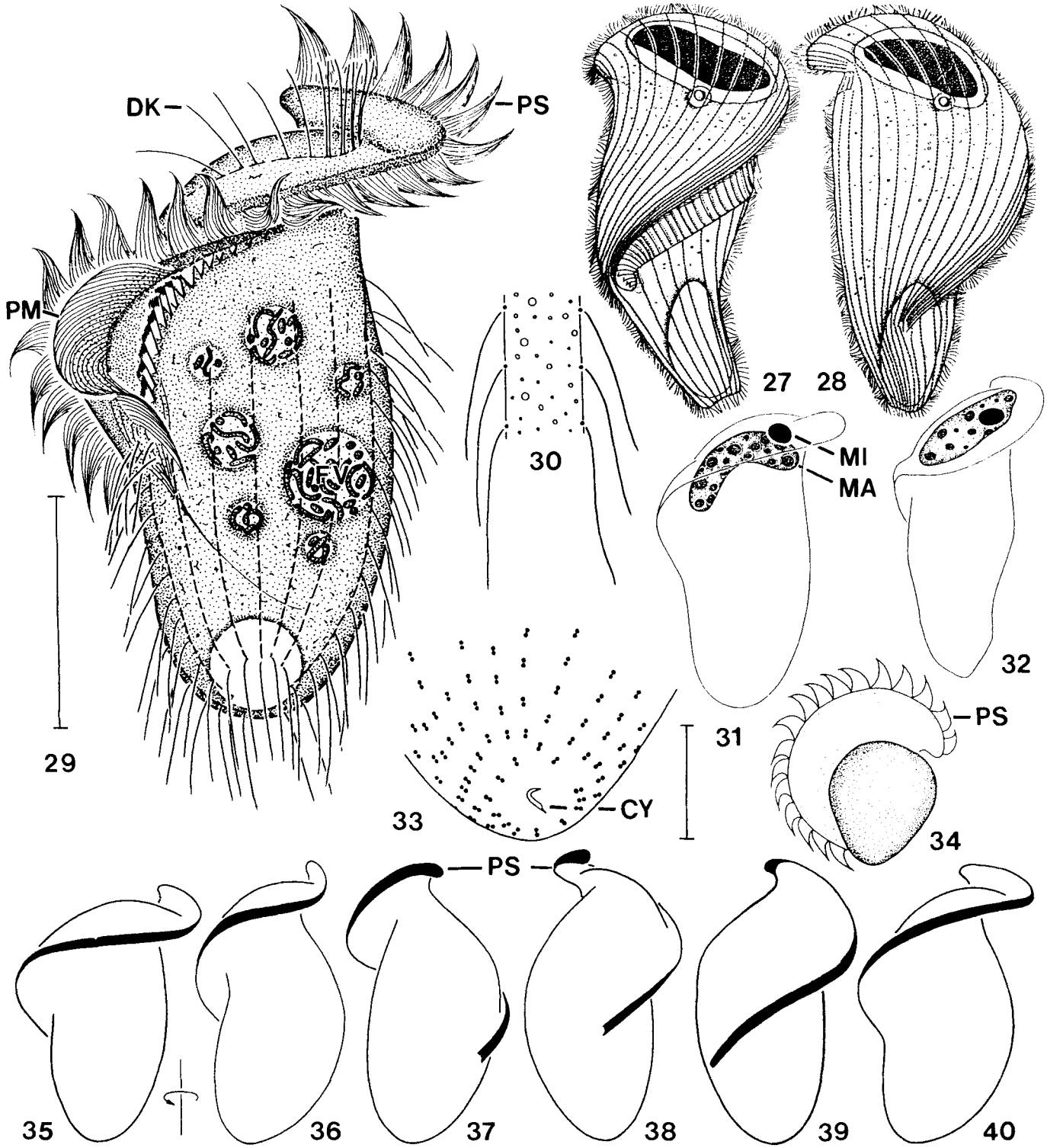


Fig. **27–40**. *Metopus inversus* from life (29–31, 34–40), preserved with saturated mercuric chloride (27, 28, from [30]) and after protargol impregnation (32, 33). **27, 28**. Right lateral and dorsal view of specimens from type population, length 90–105 μm. **29, 31**. Ventral view and nuclear apparatus, which is invariably in the preoral dome, of a representative specimen from Namibian neotype population. **30**. Surface view showing loosely arranged, inconspicuous cortical granules. **32**. Ventral view of a slender specimen. **33**. Infraciliature of posterior ventral side. The dorsal kineties extend across the pole to a circular patch containing the cytopyge. **34**. Oblique posterior polar view showing dome brim widely projecting above ventral and lateral body surface. The cilia of the perizonal stripe form conspicuous metachronal waves. **35–40**. Body shapes during 360° clockwise rotation about main body axis, beginning with a typical ventral aspect (redrawn from video records of a single specimen). CY, cytopyge; DK, dome kinety; FV, food vacuole; MA, macronucleus; MI, micronucleus; PM, paroral membrane; PS, perizonal ciliary stripe. Bars = 30 μm (Fig. 29) and 10 μm (Fig. 33).

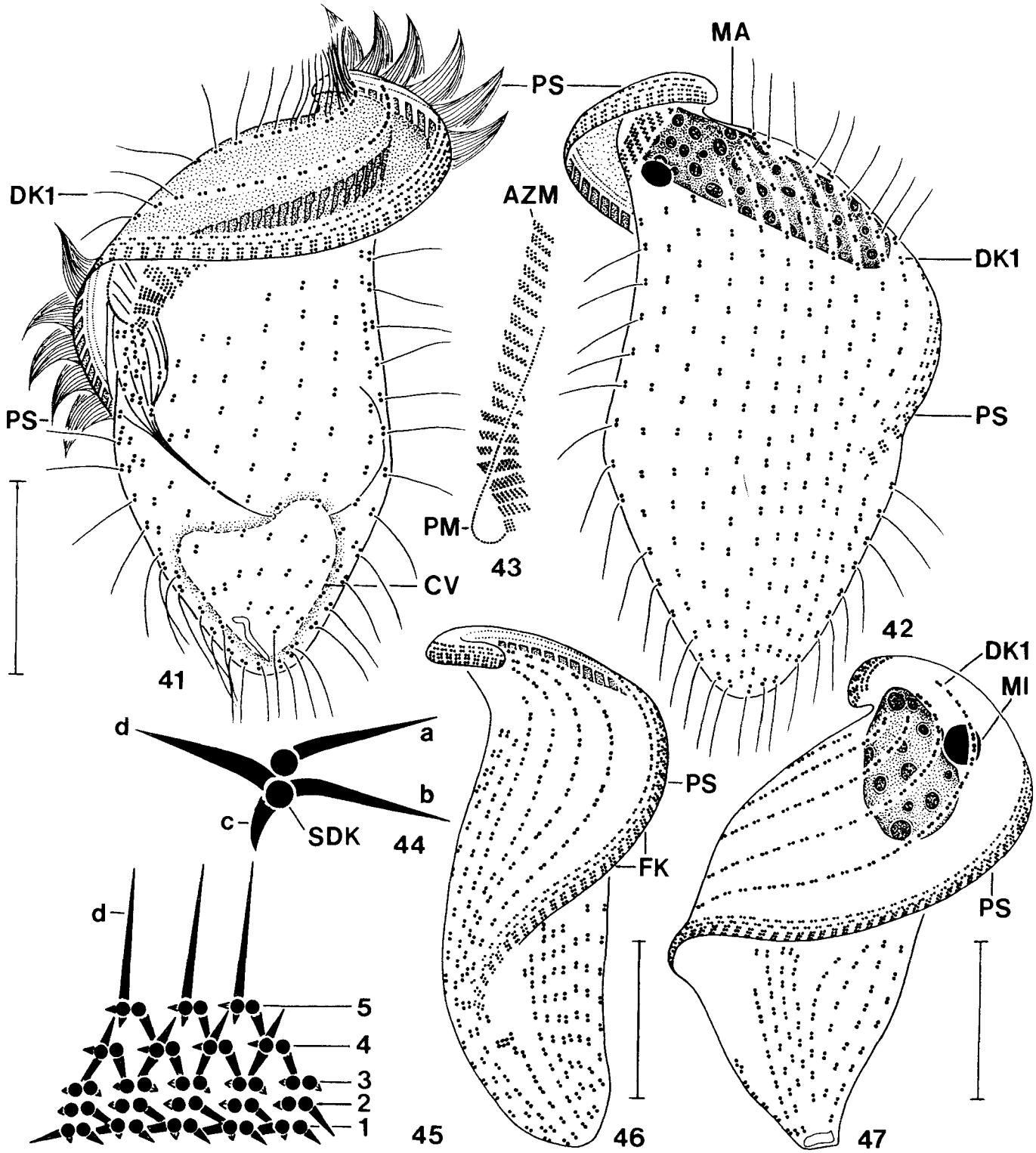


Fig. **41–47**. *Metopus inversus*, infraciliature and nuclear apparatus after protargol (41–43, 46, 47) and silver carbonate (44, 45) impregnation. **41, 42**. Ventral and dorsal view of a representative specimen. Note that dome kinety 1 terminates near posterior end of perizonal stripe. **43**. Oral structures. The membranelle structure is different in the long distal and the short proximal portion of the adoral zone. **44, 45**. Structures associated with somatic dikinetids and dikinetids in perizonal stripe, which consists of five particularly arranged ciliary rows. Structure (d) is distinctly elongated in row 5 (cp. Fig. 49). **46**. Right side view. **47**. Ventral, oblique anterior polar view showing large preoral dome. a–d, structures associated with somatic dikinetids (for details, see Discussion and Fig. 83–85); AZM, adoral zone of membranelles; CV, contractile vacuole; DK1, dome kinety 1; FK, "false" kineties formed by perizonal rows 1–3; MA, macronucleus; MI, micronucleus; PM, paroral membrane; PS, perizonal stripe; SDK, somatic dikinetid; 1–5, perizonal kineties. Bars = 20 μm.

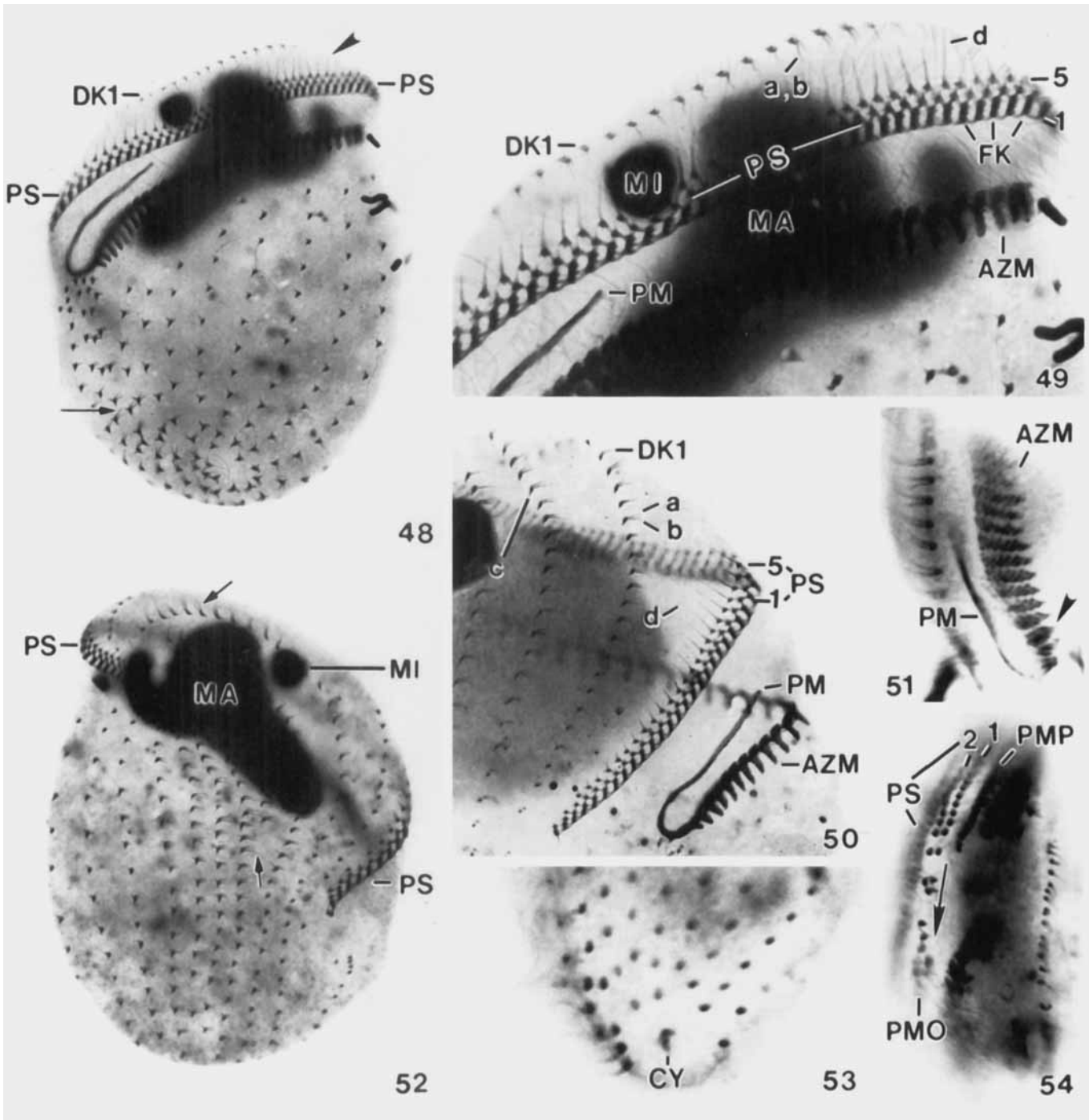


Fig. **48–54**. *Metopus inversus,* infraciliature of morphostatic (48–53) and dividing (54) specimens after silver carbonate (48–50, 52) and protargol (51, 53, 54) impregnation. Figures without scale bars since the applied technique causes unavoidable distortions of the cells, making measurement meaningless. **48, 52**. Ventral and dorsal side of same, heavily squashed specimen. The length of the kinetid associates depends on the body region: structures (a, b, c) are longest in the postcytostomial ciliary rows and in the anterior half of the dorsal kineties (arrows); structure (d) is elongated in the anterior dome area and in the mid-portion of perizonal row 5 (arrowhead). **49**. High magnification of the perizonal stripe (cp. Fig. 45, 48), which has a peculiar texture due to the kinetid associates and the "false" kineties formed by rows 1–3. **50**. Anterior right dorsal side showing details of the somatic and oral infraciliature. **51**. Oral structures. The proximal membranelles (arrowhead) appear shortened because the adoral zone performs a slight clockwise rotation (cp. Fig. 43). **53**. Posterior ventral side with cytopyge. **54**. Right lateral view of a late divider showing the formation of the opisthe's paroral by dikinetids of parental perizonal rows 1 and 2 (arrow; cp. Fig. 78). a–d, structures associated with a somatic dikinetid (for details, see Discussion and Fig. 83–85); AZM, adoral zone of membranelles; CY, cytopyge; DK1, dome kinety 1; FK, "false" kineties formed by perizonal rows 1–3; MA, macronucleus; MI, micronucleus; PM, paroral membrane; PMO, opisthe's paroral membrane; PMP, proter's paroral membrane; PS, perizonal ciliary stripe; 1–5, perizonal ciliary rows.

nov. comb. Note that Jankowski added "sp. n." to *M. inversus* in two publications [30, 31], which appeared in the same year. However, only in one of the two studies he provided also a description; thus, this paper [31] should be considered as the place of the original description of *M. inversus*.

### Divisional morphogenesis
(Fig. 54–82)

A full morphogenetic sequence was found in *M. hasei*, whereas some stages were lacking in *M. inversus*. Most stages were seen in only two or three specimens. Thus, we depict both species, although their morphogenetic processes show only minor differences: (1) about three postcytostomial and four dorsolateral kineties participate in the formation of the adoral membranelles in *M. hasei*, about five postcytostomial and eight dorsolateral kineties are involved in *M. inversus* (Fig. 55, 56, 69, 72, 74); (2) the position of the nuclear apparatus changes distinctly in *M. inversus*, whereas it remains almost unchanged in *M. hasei* (Fig. 57, 68, 74, 80); (3) the posterior cell end of middle dividers is furrowed in *M. hasei*, while broadly rounded and slightly projecting in *M. inversus* due to the perizonal stripe, which is more distinctly curved in *M. inversus* than in *M. hasei* (Fig. 60, 61, 78, 79); (4) the preoral dome disappears earlier in *M. hasei* than in *M. inversus*, causing a distinctly different shape of early dividers (Fig. 56–59, 73–75).

**Cell shape.** Division occurs in freely motile, that is, not in encysted condition. However, dividers move slowly or lie almost motionless on the slide, very likely due to the changed cell shape and orientation of ciliary rows, as in *Caenomorpha* [39]. In early (*M. hasei*) and middle (*M. inversus*) dividers, the preoral dome disappears. This causes a fundamental change of cell shape, that is, the organisms become broadly ellipsoidal or fusiform, hardly recognizable as a *Metopus* (Fig. 56–61, 75, 78, 79). Furthermore, the posterior cell portion is moulded by the perizonal ciliary stripe, which extends to (*M. hasei*; Fig. 60, 61) or across the pole (*M. inversus*; Fig. 78, 79) in middle dividers. The reshaping of the postoral body portion commences in very late dividers, while the preoral dome is reshaped only in postdividers (Fig. 65–68, 80–82).

**Opisthe stomatogenesis and somatic division.** Division commences with the replication of dikinetids in the posterior portion of all somatic ciliary rows and progresses anteriad excluding the perizonal stripe (Fig. 55, 69–72). Both basal bodies of the individual kinetids become ciliated and slightly apart, and a new basal body is generated in front of the anterior one to form a triad; subsequently, a fourth basal body develops in front of the posterior one and then the tetrad splits into two pairs of ciliated basal bodies.

Stomatogenesis commences within about three (*M. hasei*) to five (*M. inversus*) postcytostomial and about four (*M. hasei*) to eight (*M. inversus*) dorsolateral (mainly dome) kineties, which split obliquely from the cytostomial extremity of the perizonal stripe to near posterior body end (Fig. 56–58, 72–77). The newly formed dikinetids, whose number is already sufficient to build the species-specific number of adoral membranelles (the two long rows, the third short row is added later), arrange almost perpendicularly to the kinety axis at the anterior end of the postcytostomial kineties and the posterior portion of the split kineties. They form short, oblique kinetofragments, the prospective adoral membranelles.

During the formation of the new adoral zone of membranelles, two important, concomitantly proceeding events generate and assemble the opisthe's perizonal stripe and paroral (Fig. 54, 58–61, 74–79), namely, an intrakinetal proliferation of kinetids in the perizonal rows, which thus elongate, and a conspicuous rounding of the cell reducing its length. These processes drive the perizonal stripe into the glabrous area between the opisthe's membranellar zone and the posterior end of the split parental kineties. The new paroral originates from the posterior half of perizonal rows 1 and 2, which become slightly disordered (Fig. 54, 59), while perizonal rows 3–5 remain ordered and form perizonal kineties 1′–3′ in the opisthe. Finally, the posterior half of dorsolateral (dome) kineties 1 and 2 move together becoming opisthe's perizonal ciliary rows 4′ and 5′ (Fig. 60, 61, 78). To compensate for these two ciliary rows, new ones are generated left of the opisthe's membranelle zone (Fig. 60, 78). These events lead to a shifting of kineties with a "source" of new kineties on the left of the opisthe's adoral zone of membranelles and a "sink" on the right due to the formation of the paroral membrane.

Next, the newly formed membranellar zone curves to the left and slightly anteriorly, and the division furrow becomes recognizable in mid-body, where the somatic kineties split (Fig. 63, 65). Likewise, the perizonal kineties obtain their typical pattern, and a short third row of basal bodies is added to the membranelles by triad formation, similarly to the replication of the somatic kinetids described above. The separation of the daughter cells seems to be brought about by a slight rotation of the proter relative to the opisthe (Fig. 65).

The infraciliature of the newly separated daughters is almost complete. Some minor adjustments occur in connection with the reshaping of the cell, and the caudal cilia grow out only in reshaped postdividers (Fig. 66–68, 80–82). Furthermore, the opisthe's paroral is shortened by resorption of kinetids at the anterior end (Fig. 80; also seen, but not shown in *M. hasei*).

**Nuclear division.** When division commences, the macronucleus rounds up and the micronucleus becomes large and prophasic, showing very distinct spindle microtubules and a conspicuous metaphase plate (Fig. 57, 76). In middle and late dividers, the micronucleus divides as usual, whereas the macronucleus elongates to become almost as long as the shortened cell (Fig. 62, 64–66, 79). Indeed, postdividers are easily recognized by the long (as compared to cell size), rod-shaped macronucleus (cp. Fig. 55 in [15]) and the long paroral membrane, which is partially reduced during reshaping of the cell, as described above. Finally, the macronucleus condenses and migrates to the species-specific position (Fig. 80, 82).

**Proter reorganization.** While the opisthe's paroral membrane is formed, the parental oral apparatus is partially reorganized: the pharyngeal fibres dissolve and some scattered dikinetids appear left of the proximal adoral membranelles and/or right of the paroral membrane (Fig. 59, 63, 78). When the daughters have separated, the pharyngeal fibres are rebuilt and the proximal membranelles obtain their mature configuration.

**Temporal relationship of divisional processes.** The temporal relationships between stomatogenesis, nuclear fission, and reorganization could be only roughly estimated because too few dividers were available. However, the main events in the opisthe seem to be rather strongly correlated to nuclear division and proter reorganization.

## DISCUSSION

**Kinetid structure.** Unfortunately, detailed transmission electron microscopic investigations about the somatic ultrastructure of *Metopus* are lacking. There are, however, two preliminary reports [15, 43] which provide valuable information and can be compared with the present and other [9, 18, 50] light microscopical findings. Schrenk and Bardele [43] presented a diagram of the somatic dikinetids of *M. es* (Fig. 84) and mentioned that the "postciliary microtubules do not join together to form a postciliodesma characteristic for the Heterotrichida and certain karyorelictid ciliates". These findings

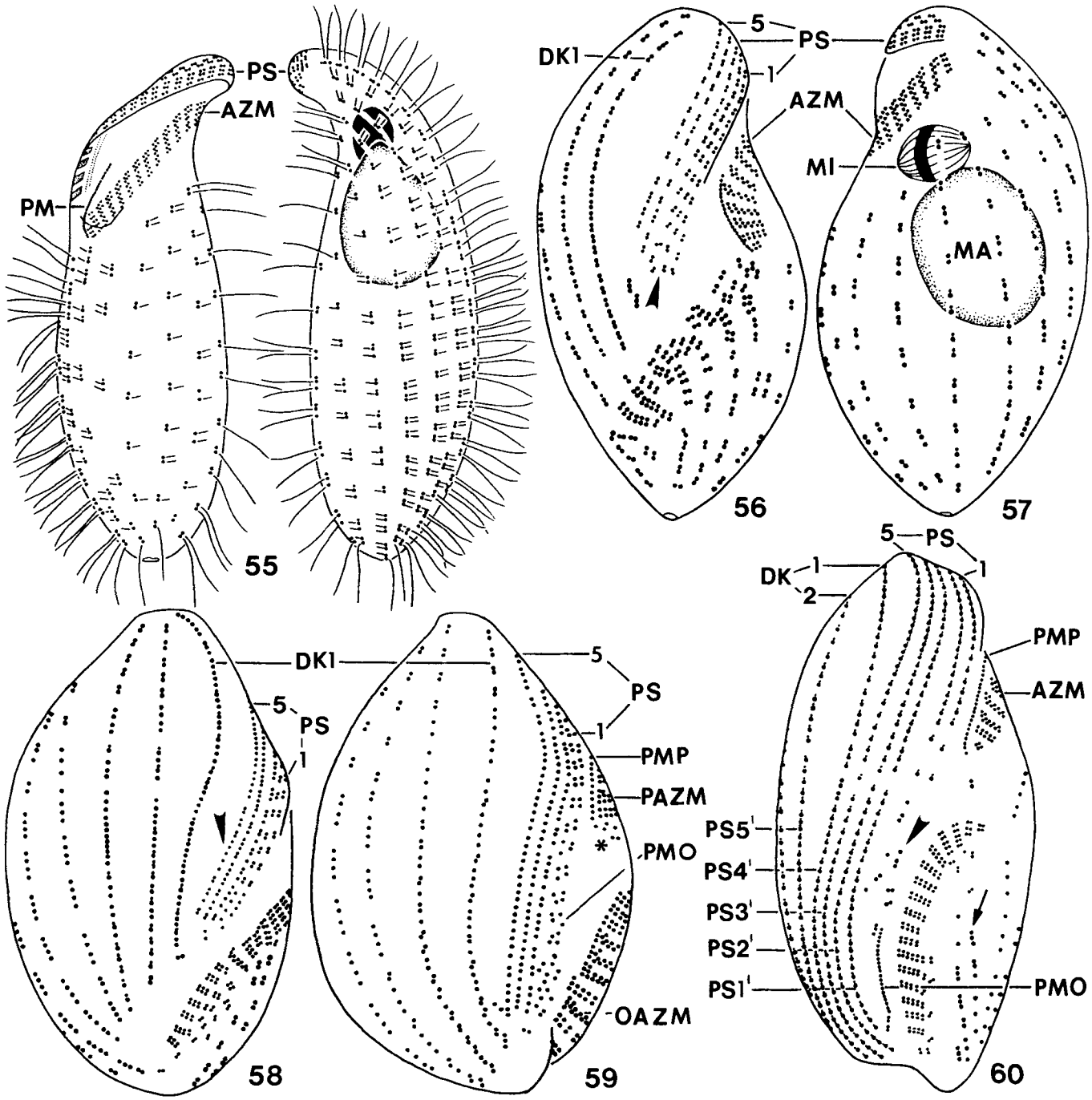


Fig. **55–60**. *Metopus hasei*, infraciliature of dividing specimens after protargol impregnation. **55**. Ventral and dorsal view of a very early divider, length 57 μm. Dikinetids become ciliated (full length of cilia shown only in marginal kineties; caudal cilia also not shown in full length) and replicate to form triads and tetrads. **56, 57**. Left and right lateral view of an early divider, length 46 μm. Dikinetids arrange perpendicularly to kinety axis and form kinetofragments at the anterior ends of three postcytostomial and the posterior portion of four split dorsal kineties. Arrowhead marks proliferating perizonal rows 1–3. **58, 59**. Right lateral view of early-middle dividers, length 43 μm and 35 μm. The perizonal stripe and the paroral membrane of the opisthe are formed by two concomitantly proceeding events, namely, an intrakinetal proliferation of kinetids in the parental perizonal rows (arrowhead), which thus elongate, and a conspicuous rounding of the cell reducing its length. These processes drive the perizonal stripe and the opisthe's paroral, which originates from perizonal rows 1 and 2, into the glabrous area between the opisthe's membranellar zone and the posterior portion of the parental kineties. Asterisk marks scattered dikinetids, indicating some reorganization of the parental oral apparatus. **60**. Right lateral view of a middle divider, length 50 μm. The cell elongates and becomes fusiform. Proter's perizonal rows 1 and 2 generate the opisthe's paroral (arrowhead), while rows 3–5 become perizonal rows 1′–3′ in the opisthe. Perizonal rows 4′ and 5′ of the opisthe are formed by the two neighbouring dorsal kineties, which move together. This loss of kineties is compensated by newly formed kineties (arrow) left of the opisthe's adoral zone. AZM, adoral zone of membranelles; DK1, 2, dome kineties; MA, macronucleus; MI, micronucleus; OAZM, opisthe's adoral zone; PAZM, proter's adoral zone; PM, paroral membrane; PMO, opisthe's paroral membrane; PMP, proter's paroral membrane; PS, perizonal stripe; PS1–5, proter's perizonal rows; PS1′–5′, opisthe's perizonal rows.

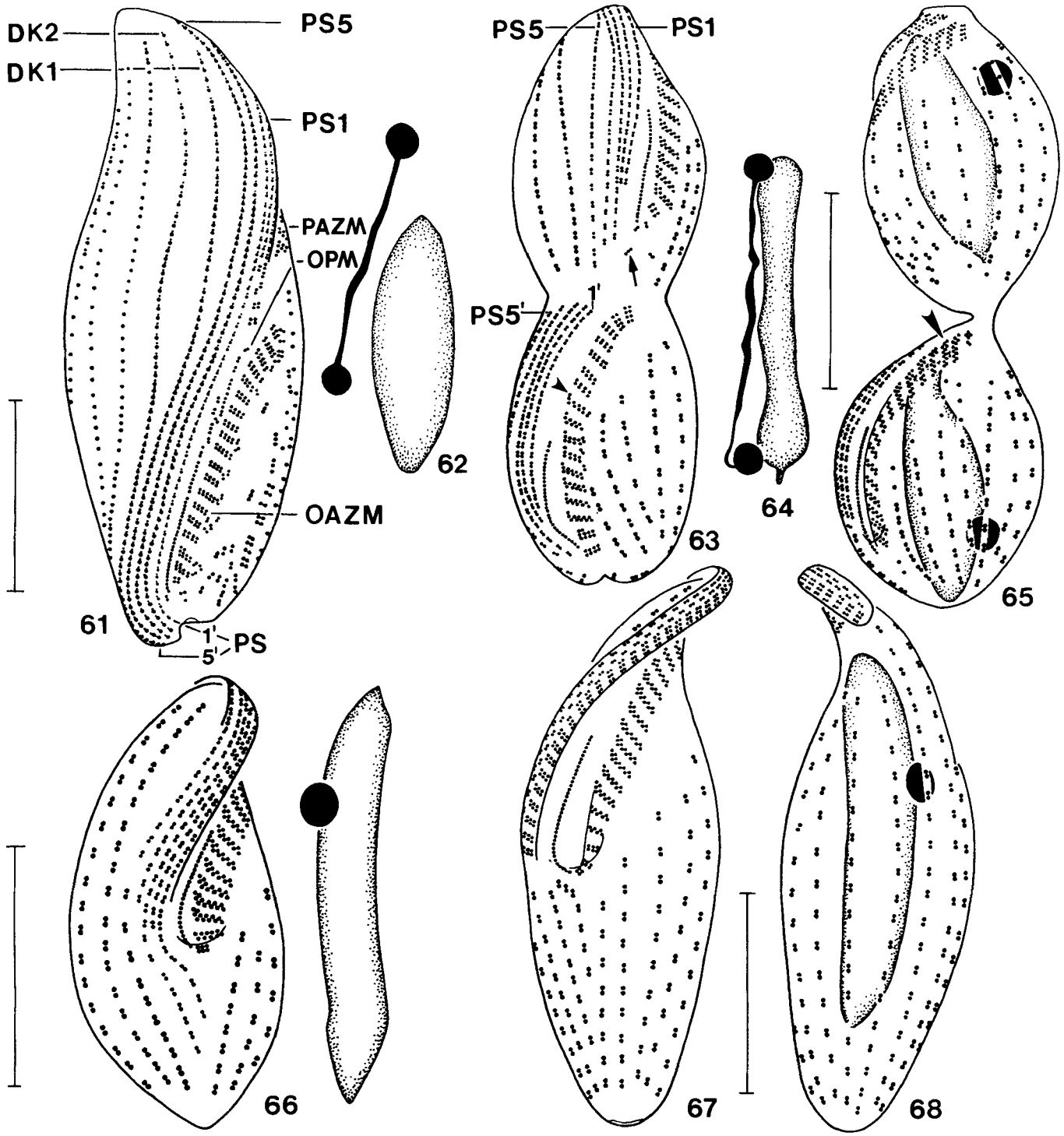


Fig. **61–68**. *Metopus hasei*, infraciliature and nuclear apparatus of dividers and postdividers after protargol impregnation. **61**, **62**. Right lateral view of a middle divider showing the fusiform body shape and the condensation of parental dome kineties 1 and 2 to opisthe's perizonal rows 4′ and 5′. In a more ventrally oriented specimen, we observed a partial reorganization of the parental paroral and the proximal adoral membranelles. **63–65**. Right lateral view of a late divider and left lateral view of a very late divider. The somatic kineties split and a third row of basal bodies is added to the opisthe's membranelles (arrowheads). Arrow marks scattered dikinetids, which are later resorbed, very likely originating from the reorganizing parental oral apparatus. **66**. Right lateral view of an early proter postdivider (recognizable by location of micronucleus). Note lack of scattered postcytostomial dikinetids and reshaping of cell. **67**, **68**. Ventral and dorsal view of a late postdivider. Postdividers are easily recognized by the long macronucleus and the long paroral membrane, which is shortened during reshaping of the cell. DK1, 2, dome kineties; OAZM, opisthe's adoral zone of membranelles; OPM, opisthe's paroral membrane; PAZM, proter's adoral zone of membranelles; PS1–5, proter's perizonal rows; PS1′–5′, opisthe's perizonal rows. Bars = 20 μm.

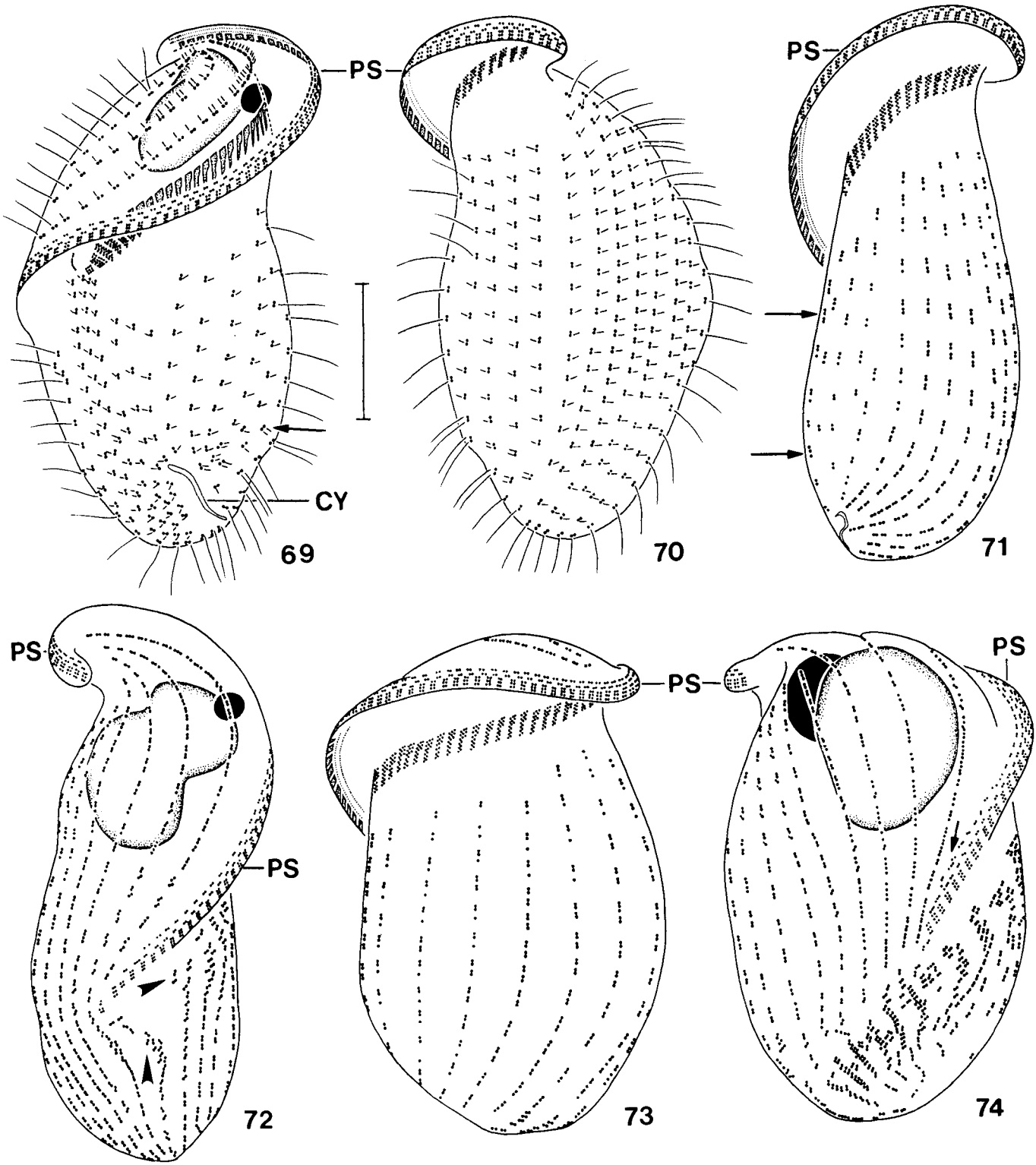


Fig. **69–74**. *Metopus inversus*, dividing specimens after protargol impregnation. **69**, **70**. Ventral and dorsal view of a very early divider. Replication of kinetids commences within the posterior portion of the ciliary rows and both basal bodies of the dikinetids become ciliated (full length of cilia shown only in marginal kineties) and slightly apart (arrow). **71**, **72**. Left and right lateral view of an early divider. All dikinetids replicate, except those in the perizonal stripe, to form triads and tetrads (arrows); dikinetids arrange perpendicularly to the kinety axis at the anterior end of about five postcytostomial kineties (arrowheads). **73**, **74**. Ventral and dorsal view of an early-middle divider. About eight dorsolateral kineties split along an oblique gradient from the cytostomial end of the perizonal stripe to near posterior body end. The dikinetids of the posterior kinety portions and of the postcytostomial ciliary rows arrange perpendicularly to the kinety axes to form kinetofragments, the prospective adoral membranelles. New basal bodies are generated within the perizonal ciliary rows (arrow) and the cell begins to round up. CY, cytopyge; PS, perizonal ciliary stripe. Bar = 20 μm for all figures.

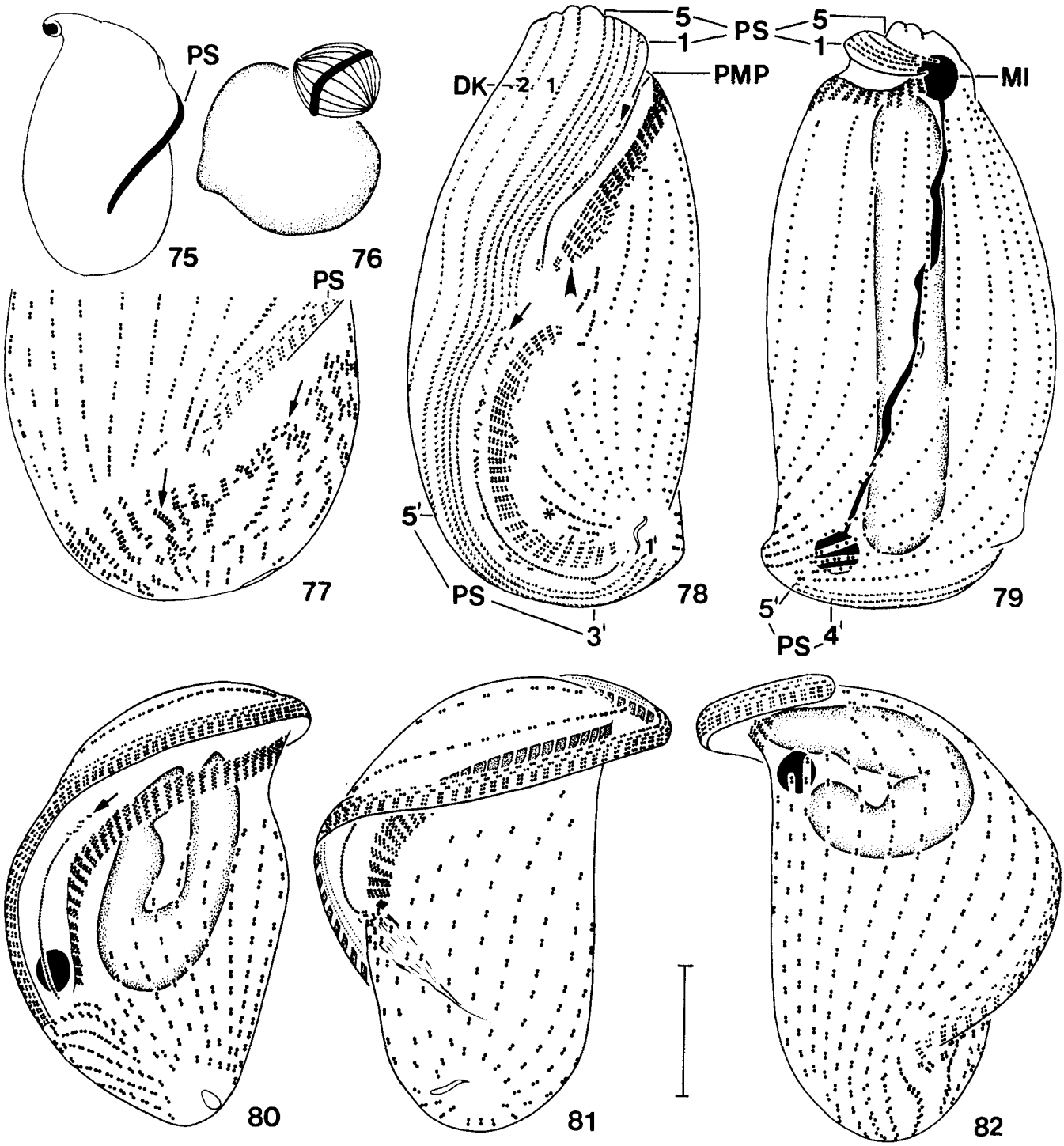


Fig. **75–82.** *Metopus inversus,* infraciliature and nuclear apparatus of dividers and postdividers after protargol impregnation. **75–77.** Right side view of an early-middle divider. The body has become ovate because of the regressing preoral dome; the micronucleus shows a conspicuous metaphase plate; new basal bodies are generated within the perizonal stripe, which thus elongates and extends into the glabrous area between the forming opisthe's membranellar zone, which consists of dikinetidal fragments (arrows), and the posterior end of the parental kineties. **78, 79.** Right and left lateral view of a middle divider. Body shape has drastically changed and driven the new adoral zone and perizonal stripe into the longitudinal body axis. Perizonal rows 1 and 2 of the proter have produced dikinetids to form the paroral membrane (arrow) of the opisthe. Likewise, proter's perizonal rows 3–5 proliferate basal bodies intrakinetally and thus elongate posteriorly to become perizonal rows 1′–3′ in the opisthe. The parental dome kineties 1 and 2 move together to become perizonal rows 4′ and 5′ in the opisthe. To compensate for these two ciliary rows, new ones are generated left of the membranellar zone (asterisk). The parental paroral and proximal adoral membranelles show some signs of reorganization (arrowheads). **80.** Ventral view of an early opisthe postdivider. Arrow marks resorbing paroral kinetids. **81, 82.** Ventral and dorsal view of a late postdivider showing reshaping of the cell. DK1, 2, dome kineties 1, 2; MI, micronucleus; PMP, proter's paroral membrane; PS, perizonal stripe; PS1–5, proter's perizonal ciliary rows; PS1′–5′, opisthe's perizonal ciliary rows. Bar = 20 μm (Fig. 77–82).

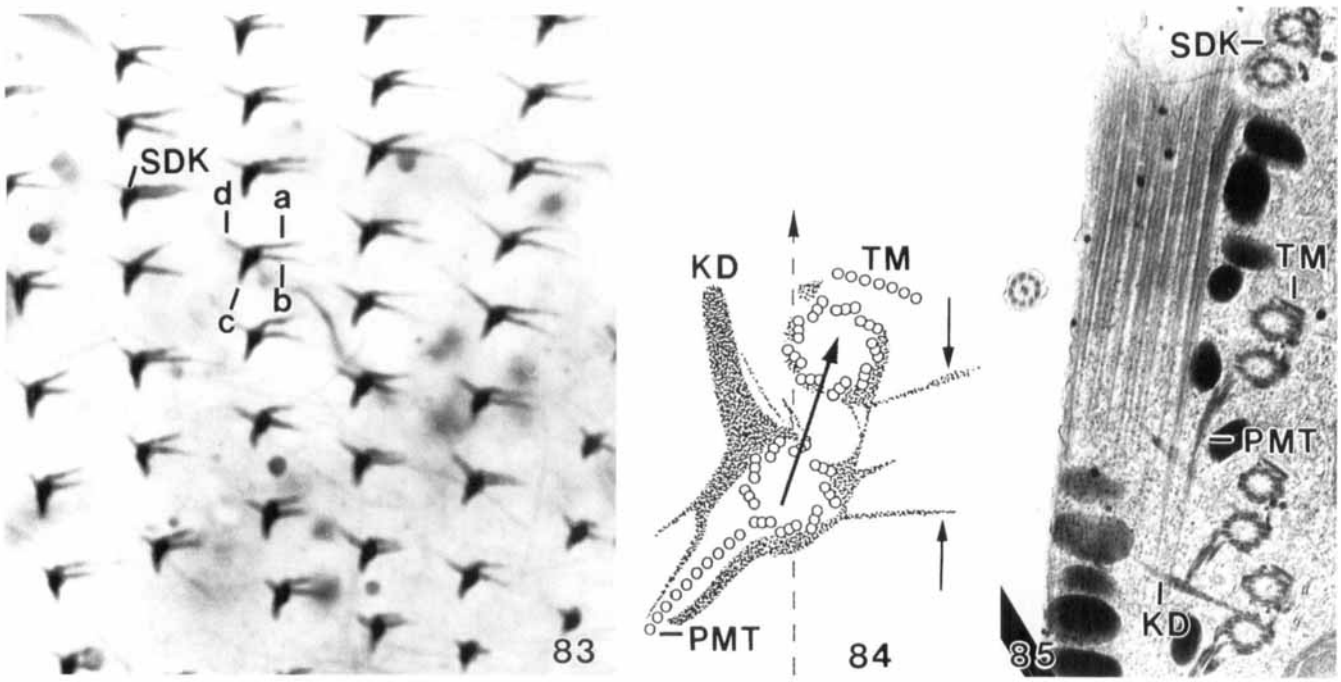


Fig. **83–85**. Comparison of light microscopic (83, *M. inversus*, silver carbonate impregnation) and electron microscopic (84, *M. es*, from [43]; 85, *M. contortus*, unpubl. micrograph kindly supplied by Finlay & Esteban) fine structures of the somatic dikinetid of *Metopus*. Although it seems possible to homologize the structures seen after silver impregnation with the electron microscopical findings, great differences, which easily give rise to misinterpretations, are obvious, that is, the silver stain shows only part of the structures. This is especially true for the conspicuous postciliary microtubule ribbon, which is very small in the silver stain [structure (c)]. On the other hand, the transversely extending, V-shaped structure (a, b) is much more prominent in the silver stain than in the electron microscope (84, arrows). The transverse microtubule ribbon is not stained at all. Only the kinetodesmal fibre [structure (d)] looks alike in the silver stain and the electron microscope. a–d, associates of somatic dikinetids as described in Result section; KD, kinetodesmal fibre; PMT, postciliary microtubule ribbon; SDK, somatic dikinetid; TM, transverse microtubule ribbon. → in Fig. 84 marks dikinetid axis, while the dashed arrow marks the axis of the kinety.

match the description by Esteban et al. [15], who characterized the somatic dikinetids of *M. contortus* and *M. palaeformis* by: "(1) An anterior kinetosome with an angled transverse ribbon formed by about 10 microtubules arranged in two sets. One set is formed by 3 microtubules and starts at the level of triplet 6. The other set includes 7 microtubules and extends over triplets 3 to 5. No kinetodesmal fibre is associated with this kinetosome. (2) A posterior kinetosome with postciliary ribbon, curved and formed from about 15 microtubules. This ribbon extends posteriorly, starting at the level of triplet 9. The kinetodesmal fibre is striated and placed at the level of triplet 6, directed laterally".

Esteban et al. [15] gave no information about the length and arrangement of the postciliary microtubules. However, they sent us a TEM-micrograph, which shows clearly long postciliary microtubule ribbons forming a single layer between the somatic kineties (Fig. 85). This is sustained by silver carbonate micrographs from *Metopus es* [9]. They show long fibres, which originate at the right side of the kinetids and extend obliquely posteriad between the ciliary rows. Accordingly, these structures cannot be kinetodesmal fibres, as stated by Decamp [9], but are very likely postciliary microtubule ribbons. Taking together the evidences from Decamp [9], Esteban et al. [15], and Schrenk and Bardele [43], it is obvious that the metopid somatic dikinetid is highly different from that of typical heterotrichs. Heterotrichs lack kinetodesmal fibres and have stacked postciliary microtubule ribbons, which form a distinct, protargol-affine fibre (postciliodesma) close to the right of the kineties [22, 40, 50]. Given the incompleteness of the ultrastructural data, any detailed comparison with other kinetids could be misleading. However, the strongly developed and plate-like arranged postciliary microtubules are reminiscent of haptorid kinetids, for instance, *Spathidium* [54].

The electron microscopical findings [15, 43] are very different from the present (Fig. 7, 21, 44, 48–50, 52, 83) and most previous [18, 50] light microscopical data, although it seems possible to relate the structures revealed by the light and electron microscope (Fig. 83–85): structures (a, b), which are very prominent in the silver stains, are very likely related to the inconspicuous fibro-granular material shown in Schrenk and Bardele's [43] diagram; structure (c) is very likely the basal part of the postciliary microtubule ribbon; and structure (d) is the kinetodesmal fibre, according to its location and orientation; the transverse microtubule ribbon is obviously not stained. There can be no doubt that the silver stains show only part of the somatic fibrillar system. In spite of this, it seems valuable to describe minutely the structures recognizable, not only to avoid misinterpretations but also to give electron microscopists some information about specializations in various body regions.

**Comparative morphogenesis.** The metopid morphogenesis shows four main features: (1) the body shape changes drastically so that the infraciliature becomes meridionalized, (2) the adoral membranelles originate as kinetofragments at the end of split somatic kineties, (3) the paroral membrane is generated by two somatic kineties from the perizonal stripe, and (4) the opisthe's perizonal stripe originates from three dividing parental perizonal kineties and two newly added dorsal ciliary rows. Thus, the metopid stomatogenesis is entirely somatic, that is, parental oral structures are not involved in any stage of the process. This is characteristic of the parakinetal and telokinetal

stomatogenic modes, which occur mainly in heterotrichs, tetrahymenine hymenostomes, gymnostomes, prostomes, and colpodids [24]. Accordingly, groups which have a buccokinetal (e. g. peniculine hymenostomes, like *Paramecium* [24]; scuticociliates, like *Uronema* [24]; loxodids [4]) or mixokinetal (e. g. nassulids [13]) stomatogenesis, where parental oral structures are involved in the opisthe's mouth formation [24], will be rarely considered in the following discussion. Likewise excluded are groups, such as oligotrichs and some hypotrichs, which have an apokinetal stomatogenesis, where the oral anlage has no apparent preassociation with either somatic kineties or the parental buccal apparatus [24].

Parakinetal stomatogenesis typically involves an anarchic field of basal bodies, which splits longitudinally and unequally: the larger left portion produces the adoral membranelles, the smaller right forms the paroral membrane. Representative examples are *Blepharisma* [1] and *Tetrahymena* [2]. Thus, *Metopus,* which forms the oral structures in a very different way, cannot be closely related to these groups.

Telokinetal stomatogenesis typically involves short, dikinetidal kinetofragments, which originate within or at the end of split kineties and either form only a circumoral kinety (haptorid gymnostomes) or a circumoral kinety and adoral organelles (cyrtophorids, prostomatids, colpodids, clevelandellid heterotrichs). Several modes of telokinetal stomatogenesis have been distinguished, depending on the number and location of the stomatogenic kineties [24]. As concerns *Metopus,* the adoral membranelles are obviously formed telokinetally, specifically, pleurotelokinetally because they originate as kinetofragments subequatorially within several dorsolateral kineties, as in cyrtolophosidid and bryometopid colpodids [22] and clevelandellid heterotrichs, for instance, *Nyctotherus* [42]. In contrast, the paroral originates not telokinetally but by rearrangement of two perizonal kineties, which never had contact to parental oral structures because they originate by lateral condensation, respectively, a "source-sink-process" of somatic dorsal kineties. The *Metopus* pattern is also different from that found in clevelandellids [42] and cyrtolophosidid and bryometopid colpodids [22], which generate the paroral from dikinetids proliferated at the posterior end of split lateral kineties; thus, the forming paroral is orientated almost perpendicularly to the main body axis and close above the moulding adoral zone of membranelles. Haptorid gymnostomes have a holotelokinetal stomatogenesis, that is, all somatic kineties proliferate kinetofragments, which form the opisthe's circumoral kinety (possibly homologous to the paroral membrane); an adoral ciliature is lacking in this group [24].

Jankowski [30, 32] and Corliss [8] included only caenomorphids in the order Armophorida. Small and Lynn [44] and Puytorac [41] added metopids, obviously assuming homology of the caenomorphid and metopid perizonal stripe. Our data show that the structure, ontogenetic function, and origin of the perizonal stripe are very different in *Metopus* and *Caenomorpha,* suggesting that they are analogous structures. However, homology cannot be entirely excluded because the somatic ciliature of caenomorphids is so heavily reduced that a direct comparison with the holotrichously ciliated metopids is difficult. The arrangement of the dikinetids and the fibrillar associates of the perizonal stripe look rather different in *Metopus* (Fig. 45, 49) and *Caenomorpha* [10, 16, 45], although a detailed comparison must await electron microscope investigations. The metopid perizonal stripe produces only the opisthe's paroral membrane, whereas the caenomorphid stripe generates the paroral, the adoral membranelles, and even the new perizonal stripe for the opisthe [39]. Specifically, the adoral membranelles are produced by *posterior* proliferation of the stripe kineties, while the paroral originates from the newly formed adoral membranelles by *anterior* proliferation of dikinetids. The stripe itself is duplicated by *anterior* proliferation of the parental stripe kineties.

**Phylogenetic considerations.** The kinetid structure, ontogenesis, and gene sequences [37, 38] show that *Metopus* is quite different from other classical heterotrichs, with which it was classified for more than 100 years due to the conspicuous adoral zone of membranelles [41, 48]. On the other hand, we could not find a specific ontogenetical feature that would support the gymnostome or clevelandellid relationships indicated by sequence data [14, 27, 37, 38]. Certainly, the somatic stomatogenesis supports, or at least does not contradict, such relationships, but is highly ambiguous because it occurs also in other groups, such as cyrtophorids, prostomatids, colpodids, and caenomorphids [24]. *Nyctotherus* and *Bryometopus,* for instance, have a pleurotelokinetal stomatogenesis [42, 55], and *Colpoda* and *Caenomorpha* change body shape like *Metopus* during morphogenesis [22, 39]. Possibly, detailed transmission electron microscope investigations on the morphology and the morphogenetic processes will provide deeper insights, as they did in other groups [3, 35].

Metopids are morphologically and ontogenetically as distinct as heterotrichs and armophorids. Thus, they should have the same (ordinal) rank. Jankowski [32] already raised the Metopidae to subordinal level within the order Heterotrichida. We suggest removing the Metopina from the Heterotrichida, to give them ordinal rank (Metopida Jankowski, 1980 n. stat.), and to place them as incertae sedis in the subphylum Intramacronucleata Lynn, 1996 [36]. The main characteristics of the order Metopida are: (1) somatic dikinetids (exact structure not yet known); (2) a usually conspicuous adoral zone of membranelles which is generated pleurotelokinetally; (3) a perizonal stripe composed of five specialized kineties, two of which produce the opisthe's paroral membrane; (4) the opisthe's perizonal stripe originates from three dividing parental perizonal kineties, and by lateral condensation of two dorsal ciliary rows.

## ACKNOWLEDGMENTS

This study was supported by the Austrian Science Foundation (FWF, Project P 12367-BIO). The technical assistance of Brigitte Moser and Mag. Eric Strobl is greatly acknowledged.

## LITERATURE CITED

1. Aescht, E. & Foissner, W. 1998. Divisional morphogenesis in *Blepharisma americanum, B. undulans,* and *B. hyalinum* (Ciliophora: Heterotrichida). *Acta Protozool.,* **37**:71–92.

2. Bakowska, J., Nelsen, E. M. & Frankel, J. 1982. Development of the ciliary pattern of the oral apparatus of *Tetrahymena thermophila. J. Protozool.,* **29**:366–382.

3. Bardele, C. F. 1989. From ciliate ontogeny to ciliate phylogeny: a program. *Boll. Zool.,* **56**:235–244.

4. Bardele, C. F. & Klindworth, T. 1996. Stomatogenesis in the karyorelictean ciliate *Loxodes striatus*: a light and scanning microscopical study. *Acta Protozool.,* **35**:29–40.

5. Bernhard, D., Leipe, D. D., Sogin, M. L. & Schlegel, K. M. 1995. Phylogenetic relationships of the Nassulida within the phylum Ciliophora inferred from the complete small subunit rRNA gene sequences of *Furgasonia blochmanni, Obertrumia georgiana,* and *Pseudomicrothorax dubius. J. Euk. Microbiol.,* **42**:126–131.

6. Blatterer, H. & Foissner, W. 1988. Beitrag zur terricolen Ciliatenfauna (Protozoa: Ciliophora) Australiens. *Stapfia (Linz),* **17**:1–84.

7. Corliss, J. O. 1968. The value of ontogenetic data in reconstructing protozoan phylogenies. *Trans. Am. microsc. Soc.,* **87**:1–20.

8. Corliss, J. O. 1979. The Ciliated Protozoa. Characterization, Classification and Guide to the Literature, 2nd ed. Pergamon Press, Oxford. 455 pp.

9. Decamp, O. 1996. Silver carbonate impregnation of specimens of

*Metopus es* Kahl, 1932 (Ciliophora, Heterotrichida). *Quekett J. Microsc.*, **37**:536–540.

10. Decamp, O. & Warren, A. 1997. Observations on the morphology of *Caenomorpha uniserialis* Levander, 1894 (Ciliophora, Heterotrichida) isolated from wastewater treatment plant. *Acta Protozool.*, **36**: 105–110.

11. Dragesco, J. 1996. Infraciliature et morphométrie de cinq espèces de ciliés mésopsammiques méditerranéens. *Cah. Biol. mar.*, **37**:261–293.

12. Dragesco, J. & Dragesco-Kernéis, A. 1986. Ciliés libres de l'Afrique intertropicale. *Faune tropicale*, **26**:1–559.

13. Eisler, K. & Bardele, C. F. 1986. Cortical morphology and morphogenesis of the nassulid ciliates *Furgasonia blochmanni* Fauré-Fremiet, 1967 and *Nassula citrea* Kahl, 1930. *Protistologica*, **22**:461–476.

14. Embley, T. M. & Finlay, B. J. 1994. The use of small subunit rRNA sequences to unravel the relationships between anaerobic ciliates and their methanogen endosymbionts. *Microbiology*, **140**:225–235.

15. Esteban, G., Fenchel, T. & Finlay, B. 1995. Diversity of free-living morphospecies in the ciliate genus *Metopus*. *Arch. Protistenk.*, **146**:137–164.

16. Fernandez-Galiano, D. & Fernandez-Leborans, G. 1980. *Caenomorpha medusula* Perty 1852 (Heterotrichida, Armophorina): nouvelles données sur la ciliature et l'infraciliature. *Protistologica*, **16**:5–10.

17. Fernandez-Leborans, G. 1981. Sur la phylogénie des Heterotrichina Stein 1867 des Armophorina Jankowski 1964 (Ciliophora, Heterotrichida). *C. r. hebd. Séanc. Acad. Sci., Paris*, **292**:821–824.

18. Fernández Leborans, G. & Fernández-Galiano, D. 1981. La morfología de dos especies de *Metopus*: *M. es* (O.F. Müller, 1782), Kahl, 1932, y *M. striatus*, McMurrich, 1884. *Boln. R. Soc. esp. Hist. nat.*, **79**: 83–91.

19. Foissner, W. 1981. Morphologie und Taxonomie einiger heterotricher und peritricher Ciliaten (Protozoa: Ciliophora) aus alpinen Böden. *Protistologica*, **17**:29–43.

20. Foissner, W. 1987. Soil protozoa: fundamental problems, ecological significance, adaptations in ciliates and testaceans, bioindicators, and guide to the literature. *Progr. Protistol.*, **2**:69–212.

21. Foissner, W. 1991. Basic light and scanning electron microscopic methods for taxonomic studies of ciliated protozoa. *Europ. J. Protistol.*, **27**:313–330.

22. Foissner, W. 1993. Colpodea (Ciliophora). Fischer, Stuttgart. 798 pp.

23. Foissner, W. 1995. Tropical protozoan diversity: 80 ciliate species (Protozoa, Ciliophora) in a soil sample from a tropical dry forest of Costa Rica, with descriptions of four new genera and seven new species. *Arch. Protistenk.*, **145**:37–79.

24. Foissner, W. 1996. Ontogenesis in ciliated protozoa, with emphasis on stomatogenesis. *In*: Hausmann, K. & Bradbury, P. C. (ed.), Ciliates: Cells as Organisms. Fischer, Stuttgart, Jena, New York. Pp. 95–177.

25. Foissner, W. 1998. An updated compilation of world soil ciliates (Protozoa, Ciliophora), with ecological notes, new records, and descriptions of new species. *Europ. J. Protistol.*, **34**:195–235.

26. Foissner, W., Berger, H. & Kohmann, F. 1992. Taxonomische und ökologische Revision der Ciliaten des Saprobiensystems—Band II: Peritrichia, Heterotrichida, Odontostomatida. *Informationsberichte des Bayer. Landesamtes für Wasserwirtschaft*, **5/92**:1–502.

27. Hammerschmidt, B., Schlegel, M., Lynn, D. H., Leipe, D. D., Sogin, M. L. & Raikov, I. B. 1996. Insights into the evolution of nuclear dualism in the ciliates revealed by phylogenetic analysis of rRNA sequences. *J. Euk. Microbiol.*, **43**:225–230.

28. Hirt, R. P., Dyal, P. L., Wilkinson, M., Finlay, B. J., Roberts, D. McL. & Embley, T. M. 1995. Phylogenetic relationships among karyorelictids and heterotrichs inferred from small subunit rRNA sequences: resolution at the base of the ciliate tree. *Molec. Phylogen. Evol.*, **4**:77–87.

29. International Commission on Zoological Nomenclature 1985. International Code of Zoological Nomenclature, 3rd ed. Univ. California Press, Berkeley, Los Angeles. 338 pp.

30. Jankowski, A. W. 1964a. Morphology and evolution of Ciliophora. I. The new system of sapropelebiotic Heterotrichida. *Zool. Zh.*, **43**: 503–517 (in Russian with English summary).

31. Jankowski, A. W. 1964b. Morphology and evolution of Ciliophora. III. Diagnoses and phylogenesis of 53 sapropelebionts, mainly of the order Heterotrichida. *Arch. Protistenk.*, **107**:185–294.

32. Jankowski, A. W. 1980. Conspectus of a new system of the phylum Ciliophora. *Dokl. Akad. Nauk SSSR*, **94**:103–121 (in Russian).

33. Kahl, A. 1927. Neue und ergänzende Beobachtungen heterotricher Ciliaten. *Arch. Protistenk.*, **57**:121–203.

34. Kahl, A. 1932. Urtiere oder Protozoa I: Wimpertiere oder Ciliata (Infusoria) 3. Spirotricha. *Tierwelt Dtl.*, **25**:399–650.

35. Lynn D. H. 1991. The implications of recent descriptions of kinetid structure to the systematics of the ciliated protists. *Protoplasma*, **164**:123–142.

36. Lynn, D. H. 1996. My journey in ciliate systematics. *J. Euk. Microbiol.*, **43**:253–260.

37. Lynn, D. H. & Small, E. B. 1997. A revised classification of the phylum Ciliophora Doflein, 1901. *Revta Soc. mex. Hist. nat.*, **47**:65–78.

38. Lynn, D. H., Wright, A.-D. G., Schlegel, M. & Foissner, W. 1999. Phylogenetic relationships of orders within the class Colpodea (Ciliophora), inferred from small subunit rRNA gene sequences. *J. Molec. Evol.* (in press)

39. Martin-Gonzalez, A., Serrano, S. & Fernández-Galiano, D. 1987. Cortical morphogenesis and conjugation process in *Caenomorpha medusula* (Ciliophora, Heterotrichida). *Europ. J. Protistol.*, **23**:111–121.

40. Mulisch, M., Barthlott, W. & Hausmann, K. 1981. Struktur und Ultrastruktur von *Eufolliculina* spec. Schwärmer und sessiles Stadium. *Protistologica*, **17**:285–312.

41. Puytorac, P. de 1994. Phylum Ciliophora Doflein, 1901. *Traite Zoologie*, **2(2)**:1–15.

42. Santos, S. M., Guinea, A. & Fernández-Galiano, D. 1986. Étude de l'infraciliature et du processus de bipartition chez *Nyctotherus ovalis* Leidy, 1850 (Ciliophora, Hétérotrichida). *Protistologica*, **22**:351–358.

43. Schrenk, H.-G. & Bardele, C. F. 1991. The fine structure of *Saprodinium dentatum* Lauterborn, 1908 as a representative of the Odontostomatida (Ciliophora). *J. Protozool.*, **38**:278–293.

44. Small, E. B. & Lynn, D. H. 1985. Phylum Ciliophora. *In*: Lee, J. J., Hutner, S. H. & Bovee, E. C. (ed.), An Illustrated Guide to the Protozoa. Society of Protozoologists, Allen Press, Lawrence, Kansas. Pp. 393–575.

45. Sola, A., Guinea, A., Longás, J. F. & Fernández-Galiano, D. 1990. Nouvelles données sur l'infraciliature somatique et buccale de *Caenomorpha uniserialis* Levander, 1894 (Ciliophora, Heterotrichida). *Arch. Protistenk.*, **138**:233–238.

46. Sondheim, M. 1929. Protozoen aus der Ausbeute der Voeltzkowschen Reisen in Madagaskar und Ostafrika. *Abh. senckenb. naturforsch. Ges.*, **41**:283–313.

47. Stechmann, A., Schlegel, M. & Lynn, D. H. 1998. Phylogenetic relationships between prostome and colpodean ciliates tested by small subunit rRNA sequences. *Molec. Phylogen. Evol.*, **9**:48–54.

48. Stein, F. 1867. Der Organismus der Infusionsthiere nach eigenen Forschungen in systematischer Reihenfolge bearbeitet. II. Abtheilung. 1) Darstellung der neuesten Forschungsergebnisse über Bau, Fortpflanzung und Entwickelung der Infusionsthiere. 2) Naturgeschichte der heterotrichen Infusorien. Engelmann, Leipzig. 355 pp.

49. Tucolesco, J. 1962. Études protozoologiques sur les eaux Roumaines I. Espèces nouvelles d'infusoires de la mer noire et des bassins salés paramarins. *Arch. Protistenk.*, **106**:1–36.

50. Tuffrau, M. 1968. Les structures fibrillaires somatiques et buccales chez les ciliés hétérotriches. *Protistologica*, **3** (year 1967):369–394.

51. Van Hoek, A. H. A. M., van Alen, T. A., Sprakel, V. S. I., Hackstein, J. H. P. & Vogels, G. D. 1998. Evolution of anaerobic ciliates from the gastrointestinal tract: phylogenetic analysis of the ribosomal repeat from *Nyctotherus ovalis* and its relatives. *Mol. Biol. Evol.*, **15**: 1195–1206.

52. Vuxanovici, A. 1962a. Contributii la sistematica ciliatelor (Nota II). *Studii Cerc. Biol. (Seria "biologie animala")*, **14**:331–349 (in Rumanian with French summary).

53. Vuxanovici, A. 1962b. Contributii la sistematica ciliatelor (Nota III). *Studii Cerc. Biol. (Seria "biologie animala")*, **14**:549–573 (in Rumanian with Russian and French summaries).

54. Williams, D. B., Williams, B. D. & Hogan, B. K. 1981. Ultrastructure of the somatic cortex of the gymnostome ciliate *Spathidium spathula* (O. F. M.). *J. Protozool.*, **28**:90–99.

55. Wirnsberger, E., Foissner, W. & Adam, H. 1985. Morphogenesis,

fine structure, and phylogenetic relationships of the "heterotrich" ciliate *Bryometopus atypicus* (Protozoa, Colpodea). *Annls. Sci. nat. (Zool.)*, **7**: 113–128.

56. Wright, A.-D. G. & Lynn, D. H. 1997. Monophyly of the trichostome ciliates (phylum Ciliophora: class Litostomatea) tested using new 18S rRNA sequences from the Vestibuliferids, *Isotricha intestinalis* and *Dasytricha ruminantium*, and the haptorian, *Didinium nasutum*. *Europ. J. Protistol.*, **33**:305–315.

*Received 8-14-98, 10-26-98, 12-28-98; accepted 1-20-99*

# UPCOMING MEETING

## 1st Announcement: 3rd European Congress of Protistology and 9th Conference on Ciliate Biology

**July 26–30, 1999**

The meetings will be held July 26–30, 1999 in Helsingor (Elsinore, about 40 km north of Copenhagen), Denmark. In order to receive 2nd announcement (containing more detailed information on accommodation, prices, and a tentative programme) write or fax to:

Ms Anne Holm
Marine Biological Laboratory
Strandpromenaden 5
DK-3000 Helsingor, Denmark
Fax no +45 49 26 11 65